THE JOURNAL OF COMPARATIVE NEUROLOGY 400:417–439 (1998)

Brainstem Inputs to the Ferret Medial Geniculate Nucleus and the Effect of Early Deafferentation on Novel Retinal Projections to the Auditory Thalamus

ALESSANDRA ANGELUCCI, FRANCISCO CLASCÁ, AND MRIGANKA SUR*
Department of Brain and Cognitive Sciences, Massachusetts Institute of Technology, Cambridge, Massachusetts 02139

ABSTRACT

Following specific neonatal brain lesions in rodents and ferrets, retinal axons have been induced to innervate the medial geniculate nucleus (MGN). Previous studies have suggested that reduction of normal retinal targets along with deafferentation of the MGN are two concurrent factors required for the induction of novel retino-MGN projections. We have examined, in ferrets, the relative influence of these two factors on the extent of the novel retinal projection.

We first characterized the inputs to the normal MGN, and the most effective combination of neonatal lesions to deafferent this nucleus, by injecting retrograde tracers into the MGN of normal and neonatally operated adult ferrets, respectively. In a second group of experiments, newborn ferrets received different combinations of lesions of normal retinal targets and MGN afferents. The resulting extent of retino-MGN projections was estimated for each case at adulthood, by using intraocular injections of anterograde tracers.

We found that the extent of retino-MGN projections correlates well with the extent of MGN deafferentation, but not with extent of removal of normal retinal targets. Indeed, the presence of at least some normal retinal targets seems necessary for the formation of retino-MGN connections. The diameters of retino-MGN axons suggest that more than one type of retinal ganglion cells innervate the MGN under a lesion paradigm that spares the visual cortex and lateral geniculate nucleus. We also found that, after extensive deafferentation of MGN, other axonal systems in addition to retinal axons project ectopically to the MGN.

These data are consistent with the idea that ectopic retino-MGN projections develop by sprouting of axon collaterals in response to signals arising from the deafferented nucleus, and that these axons compete with other sets of axons for terminal space in the MGN. J. Comp. Neurol. 400:417–439, 1998. © 1998 Wiley-Liss, Inc.

Indexing terms: retinal ganglion cells; plasticity; development; subcortical auditory pathways; inferior colliculus

A central question in developmental neurobiology is how axons select appropriate targets. One possibility is that axons are intrinsically determined to make specific sets of connections. Alternatively, factors extrinsic to the axons themselves might play an important role in target selection. One way of understanding the mechanisms that regulate target choice is to investigate whether the process of target selection can be experimentally modified. Previous studies in rodents (Schneider, 1973; Devor, 1975; Graziadei et al., 1979; Frost, 1981, 1982, 1986; Asanuma and Stanfield, 1990) and ferrets (Sur et al., 1988; Roe et al., 1993) have shown that, after selective brain lesions early

Grant sponsor: National Institutes of Health; Grant number: Ey 07719; Grant sponsor: March of Dimes; Grant sponsor: Fogarty International Fellowship [LGO]; Grant number: IFO5TWO4881.

Dr. Angelucci's current address: Department of Visual Science, Institute of Ophthalmology, University College London, 11-43 Bath St., London, EC1V 9EL United Kingdom.

Dr. Clascá's current address: Departamento de Morfologia, Facultad de Medicina, Universidad Autonoma, Arzobispo Morcillo s/n, 28029 Madrid, Spain.

*Correspondence to: Mriganka Sur, Department of Brain and Cognitive Sciences, Massachusetts Institute of Technology, E25–235, 45 Carleton Street, Cambridge, MA 02139. E-mail: msur@ai.mit.edu

Received 14 August 1997; Revised 15 June 1998; Accepted 28 June 1998

© 1998 WILEY-LISS, INC.

or late in development, axons can be induced to form stable terminal arbors in targets that they would not normally innervate. The occurrence of ectopic connections in vivo suggests that the process of target selection is not entirely predetermined, and might be the result of competition among different populations of axons endowed with different degrees of intrinsic "preference" for different targets. Under normal circumstances, this competition among axon populations is likely to be tightly constrained by developmental temporal and spatial factors. Selective lesions early in development constitute a powerful experimental tool to modify these temporal and spatial constraints. Thus, understanding the developmental rules that govern the establishment of anomalous connections might shed some light on how normal connections are specified.

Redirection of specific afferents to inappropriate loci has been shown to occur when normal targets are reduced in size early in development, and alternative space is created by partially deafferenting an ectopic target. Thus, for example, in rodents (Schneider, 1973; Frost, 1981, 1982) and ferrets (Sur et al., 1988; Roe et al., 1993), retinal axons were redirected to the auditory thalamus by partial neonatal ablation of the lateral geniculate nucleus (LGN) and/or the superior colliculus (SC), two main retinal targets, along with transection of the brachium of the inferior colliculus (BIC) and/or ablation of the inferior colliculus (IC) to partially deafferent the medial geniculate nucleus (MGN). It was argued that both factors, i.e., normal retinal target removal and MGN deafferentation, are necessary to induce sprouting of retinal axons into the MGN (Roe et al., 1993). However, these studies seem to indicate that the ability to form anomalous connections is limited. Only a subset of the entire population of available retinal axons could be induced to innervate novel targets. Moreover, in ferrets, novel retinal projections to the MGN were apparently formed only by one subpopulation of retinal ganglion cells, namely the W-cells (Roe et al., 1993; Pallas et al., 1994).

One possible explanation for the limited and selective induction of fibers to novel targets, is that only a subset of retinal ganglion cell axons are endowed with intrinsic plastic properties (Roe et al., 1993). An alternative explanation is that the ability of axons to innervate novel targets is determined by factors extrinsic to the axons themselves. One such factor might be the developmental age at which the experimental manipulations are performed, such that a larger proportion of axons would form novel connections if the necessary manipulations were done at earlier ages (Roe et al., 1993). Another extrinsic factor that might influence the extent of anomalous retino-MGN projections, and the one that we have examined in the present study, is the extent of the specific lesions performed at birth. In previous lesion paradigms, both removal of normal retinal targets and deafferentation of the MGN were incomplete (Frost, 1981, 1982; Sur et al., 1988; Roe et al., 1993). Specifically, ablation of the LGN was obtained indirectly by lesioning the visual cortex, thus inducing only partial degeneration of the LGN, whereas deafferentation of the MGN was performed mainly by transecting the BIC, and estimated solely by direct examination of the BIC lesion. However, over the past decade, anatomical studies on the connectivity of the cat MGN have shown that a wide diversity of brainstem afferents

Abbreviations

BC	brachium conjunctivum
BCM	marginal nucleus of the brachium conjunctivum
BIC	brachium of the inferior colliculus
BIN	nucleus of the brachium of the inferior colliculus
CAE	locus coeruleus
cIC	contralateral inferior colliculus
CP	cerebral peduncle
Cu	cuneiform nucleus
CUN	cuneate nucleus
DMV	dorsal motor nucleus of the vagus
DR	dorsal nucleus of the raphe
FTC	central tegmental field
FTG	magnocellular tegmental field
FTL	lateral tegmental field
FTP	paralemniscal tegmental field
GR	gracile nucleus
IC	inferior colliculus
iIC	ipsilateral inferior colliculus
IOd	dorsal nucleus of the inferior olive
IOm	medial nucleus of the inferior olive
LC	linear central nucleus of the raphe
LGd	dorsal lateral geniculate nucleus
LGN	lateral geniculate nucleus
LGv	ventral lateral geniculate nucleus
LLD	dorsal nucleus of the lateral lemniscus
LLV	ventral nucleus of the lateral lemniscus
LP	lateral posterior thalamic nucleus
LRN	lateral reticular formation
LSO	lateral nucleus of the superior olivary complex
MGN	medial geniculate nucleus
MGd	dorsal division of the medial geniculate nucleus
MGm	medial division of the medial geniculate nucleus
MGv	ventral division of the medial geniculate nucleus
ML	medial lemniscus
MM	mammillary nucleus
MSO	medial nucleus of the superior olivary complex
OT	optic tract
P	pyramidal tract
PAG	periaqueductal gray
PBG	parabigeminal nucleus
Po	lateral part of the posterior group of thalamic nuclei
PoM	medial division of the posterior nuclear thalamic complex
PR	paramedian reticular formation
PT	pretectal nuclei
RGCS	retinal ganglion cells
RN	Csred nucleus
RTN	reticular thalamic nucleus
SAG	nucleus sagulum
SC	superior colliculus
SCC	commissure of the superior colliculus
SCd	deep layers of the superior colliculus
SCs	superficial layers of the superior colliculus
Sg	suprageniculate nucleus
SN	substantia nigra
SO	superior olivary complex
ST	nuclei of the solitary tract
STT	spinothalamic tract
T	nucleus of the trapezoid body
VB	ventrobasal thalamic complex
vl	pars lateralis of the ventral division of the medial geniculate nucleus
VN	vestibular nuclei
V4	4th ventricle
3	oculomotor nuclei
5P	principal sensory trigeminal nerve
5SP	spinal nucleus of the trigeminal nerve
5ST	spinal trigeminal tract
7g	genu of the facial nerve
12	hypoglossal nerve

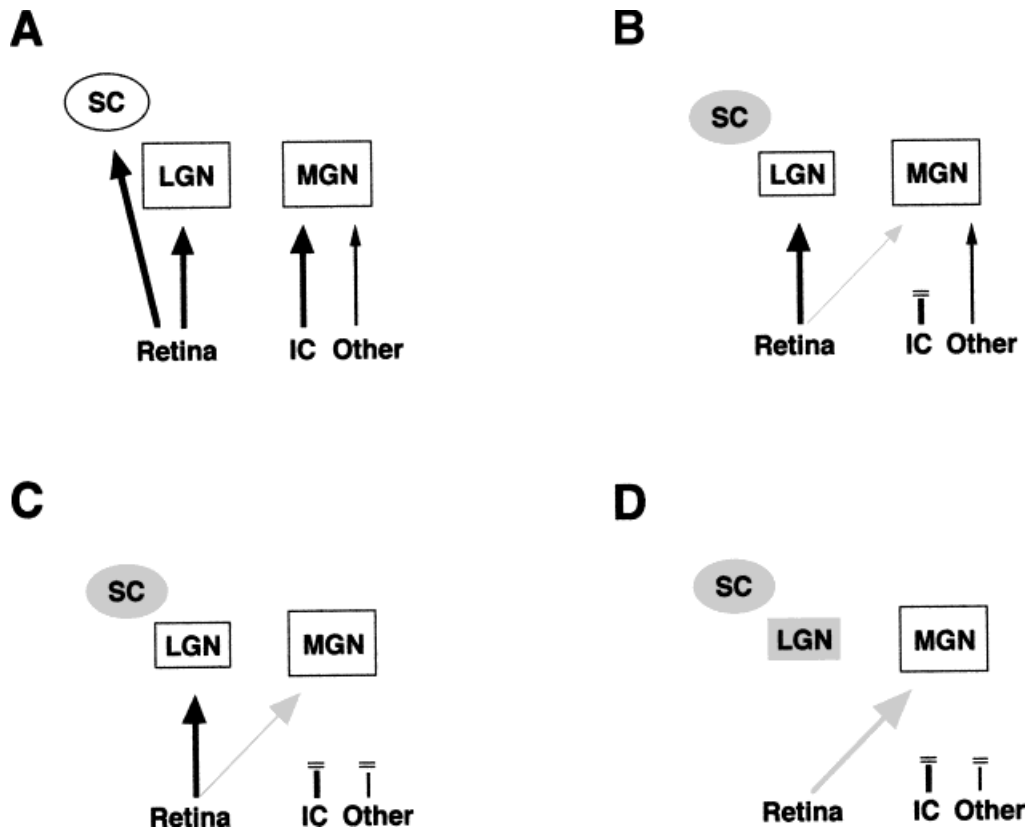

Fig. 1. Hypothetical factors affecting the quantity of anomalous retinal projections to the medial geniculate nucleus (MGN). Arrows represent axonal projections. Ablated nuclei are represented as gray areas. Double horizontal lines indicate sectioning of ascending fibers to the MGN. **A:** Projections in normal animals. The retina projects mainly to the superior colliculus (SC) and lateral geniculate nucleus (LGN). By analogy with the cat MGN, in addition to brachial afferents from the ipsilateral inferior colliculus (IC), the ferret MGN might also receive nonbrachial afferents from other auditory and nonauditory brainstem nuclei (other). **B:** Experimental paradigm used in previous studies to induce retinal projections to the MGN. If the SC is ablated at birth, the LGN reduced in size, and alternative terminal space is created by removing the ipsilateral IC, or sectioning fibers ascending from it (namely the brachium of the IC), a small proportion of retinal axons (gray arrow) are induced to innervate the MGN. **C:** If extent of MGN deafferentation affects the amount of anomalous retinal connections, then removing all or most of the inputs to the MGN should induce a larger fraction of retinal axons (gray arrow) to sprout into this nucleus. **D:** If both extent of MGN deafferentation and removal of normal retinal targets affect the quantity of retino-MGN projections, then complete removal of the SC, LGN, and MGN afferents should induce an even larger proportion of retinal cells to project to the auditory thalamus (arrow).

reach the normal MGN (reviewed in Winer, 1992), raising the possibility that many afferents might be spared by the BIC lesion alone.

Thus, in the first part of this study, we have carried out a systematic analysis of the sources and pathways of inputs to the MGN in normal adult ferrets (Fig. 1A) and in adult ferrets that received different types of neonatal lesions aimed at deafferenting this nucleus.

In a second group of experiments, we have reexamined the relative influence of normal retinal target removal and MGN deafferentation on the extent of the novel retinal projection to the auditory thalamus. Specifically, our working hypotheses are illustrated in Figure 1B–D. If deafferentation of the MGN is at least one important factor that influences the quantity of anomalous retinal projections to this nucleus, then partial ablation of MGN afferents and normal retinal targets should induce a smaller fraction of retinal axons to innervate the MGN (Fig. 1B) than partial ablation of normal retinal targets and complete removal of MGN afferents (Fig. 1C). No difference in the extent of the novel projection should be observed after partial or complete removal of MGN afferents, if deafferentation of this nucleus were not a crucial factor. If ablation of normal retinal targets also influences the extent of retinal projections to MGN, then complete ablation of normal retinal targets, along with complete MGN deafferentation, should further increase the amount of retino-MGN projections (Fig. 1D).

Our results confirm the hypotheses of Figure 1A–C but, surprisingly, not that of Figure 1D. Although this conclusion is tempered by the technical difficulty of deafferenting the MGN without affecting the SC, these data indicate that, at least for the retinofugal projections we have described, the extent of MGN deafferentation is significantly more important in regulating novel projections to this target than the extent of normal target removal.

MATERIALS AND METHODS

Animals

The animals used were pigmented ferrets (*Mustela putorius furo*, family Mustelidae, order Carnivora) bred in our colony or purchased from a vendor (Marshall Farms, North Rose, NY). A total of 22 adult ferrets were used. Most of these animals (n = 20) had received neonatal brain lesions (see below), whereas two normal animals were used as controls. All the surgical and experimental procedures were approved by the Animal Care and Use Committee of the Massachusetts Institute of Technology and were carried out under the guidelines for animal use established by National Institutes of Health.

Injections of retrograde tracers in the MGN to label auditory thalamic afferents

To identify sources of inputs to the MGN in normal ferrets and ferrets in which the MGN had been deafferented at birth (see below), retrograde tracers were injected in two normal and three lesioned adult animals. In adult ferrets that had been operated at birth, some degree of displacement of the various thalamic nuclei was usually observed, making it difficult to reach the MGN under stereotaxic guidance. For this reason, we developed a surgical protocol to perform intrathalamic tracer injections under direct visual guidance. After prophylactic administration of atropine (0.04 mg/kg intramuscularly [i.m.]), dexamethasone (0.7 mg/kg i.m.), and amoxicillin (20 mg/kg i.m.), the animals were preanesthetized with a mixture of ketamine (30 mg/kg i.m.) and xylazine (1.5 mg/kg i.m.), intubated with an endotracheal tube, and placed in a stereotaxic apparatus. Anesthesia was subsequently maintained with 1–2% isofluorane in a 1/1 mixture of nitrous oxide and oxygen. Heart and respiration rates were monitored, body temperature was maintained at 38°C, and lactated Ringers' solution (1–2 cc/kg per hour) was administered intravenously. Under sterile conditions and microscopic observation, the skin and head muscles were incised, and a unilateral craniotomy was performed. After durotomy, to protect the cortex, small pieces of hemostatic gelatin sponge were inserted between the skull and the underlying cortical surface around the craniotomy, and the cortex was kept moist by repeated irrigation with normal saline. The occipital cortex was then gently lifted until the lateral and medial geniculate nuclei became visible. A micropipette (20–30 μm inside tip diameter) sealed to a 1-μl Hamilton microsyringe was lowered into the caudal pole of the MGN, and a mixture of 3% wheat germ agglutinin conjugated to horseradish peroxidase (WGA-HRP; Sigma, St. Louis, MO) and 20% HRP (Sigma) in saline (150–250 nl) was pressure injected. On completion of surgery, the craniotomy was closed with laboratory sealing film (parafilm) sealed to the skull with dental acrylic, and the muscle and skin were sutured. Throughout the postoperative period, dexamethasone (0.7 mg/kg) and amoxicillin (10–15 mg/kg) were administered. After 2–3 days of survival, the animals were euthanized with sodium pentobarbital (80 mg/kg intraperitoneally [i.p.]) and transcardially perfused with saline for 3–5 minutes, followed by a fixation solution of 1% paraformaldehyde and 1.25% glutaraldehyde in 0.1 M phosphate buffer, pH 7.4 (PB), for 30 minutes. The excess fixative was then removed from the tissue by perfusing with 5–10% sucrose in PB for 30 minutes. The brains were blocked stereotaxically, removed from the skull, cryoprotected, and sectioned with a freezing microtome at 50 μm in the coronal plane. In two of the lesioned animals, the cervical spinal cord was also removed and was sectioned in the parasagittal plane. In all cases, every fourth section was processed by using tetramethylbenzidine (TMB) to reveal HRP according to the protocol of Mesulam (1978) and counterstained with thionin or neutral red. For cytoarchitectonic identification of brain structures, adjacent series of sections were stained for Nissl substance or cytochrome oxidase (Wong-Riley, 1979). Sections were mounted, air dried, dehydrated, and coverslipped.

Neonatal surgery to induce retinal innervation of the MGN

To test whether the extent of the novel retinal projection to the auditory thalamus correlates with the extent of MGN deafferentation and/or the extent of removal of normal retinal targets, we used different combinations of lesions in different animals (n = 20). Generally, lesions were combined as follows: (1) moderate deafferentation of the MGN with moderate or extensive removal of the principal retinal targets, and (2) extensive MGN deafferentation with moderate or extensive removal of retinal targets. Lesions aimed at reducing or completely removing the principal retinal targets included partial or complete ablation of one or several of the following brain structures: (1) the visual cortex, to induce partial retrograde degeneration of the LGN; (2) the LGN, directly; (3) the pretectal nuclei (PT); (4) the superficial layers of the SC. Lesions aimed at reducing brainstem inputs to the MGN included partial or complete transection of the BIC, the main ascending pathway to the MGN, combined with one or several of the following: (1) transection of ipsilateral extrabrachial afferents, (2) ablation of contralateral brainstem afferents, (3) removal of the deep layers of SC, (4) ipsilateral or bilateral ablation of the IC. (See Results section and Figs. 5, 8 for a detailed description of the type and extent of lesions in each case.)

Surgical procedures were similar to those described previously (Sur et al., 1988; Angelucci et al., 1997). Briefly, 1 day after birth (postconception day 43), ferret kits were anesthetized by deep hypothermia. The scalp was incised along the sagittal midline, and a small craniotomy was made in the occipital bone to expose the mesencephalon and the occipital pole of the cerebral hemispheres. The SC and, when needed, the IC and the occipital (presumptive visual) cortex were directly cauterized. To directly ablate the LGN and PT, the caudal aspect of the diencephalon was exposed by gently lifting the occipital cortex, and the caudodorsal thalamus was cauterized. To transect the BIC, the lateral third of the mesencephalon was coronally sectioned at the midcollicular level. To sever the ipsilateral extrabrachial afferents to the MGN, the lateral mesencephalic cut was extended medial and ventral to the BIC. The contralateral auditory brainstem inputs to the MGN were severed by cauterizing the commissure of the SC (SCC) and the contralateral IC (cIC; see Results section). All lesions were made unilaterally, except in five animals that received bilateral lesions. On completion of surgery, the skin was sutured with reabsorbable 5–0 suture. The kits were revived under a heat lamp and returned to the jill for rearing to adulthood. At adulthood (>4 months after birth), to characterize the most effective combination of lesions to deafferent the MGN, three animals received

injections of retrograde tracers in the MGN (as described above). All the remaining animals received intraocular injections of anterograde tracers (see below).

Intraocular injections of anterograde tracers to label retinal projections to the MGN

To estimate the extent of retino-MGN projections induced by different combinations of neonatal lesions, a first group of lesioned animals (n = 15) received bilateral intraocular injections of WGA-HRP (4–5% in saline, 8–10 µl) at adulthood. To measure axon diameters of the population of retinal ganglion cells projecting to the MGN, a separate group of bilaterally lesioned animals (n = 2) received injections of cholera toxin subunit B (CTB, List Labs, Campbell CA; 1% in distilled water, 10 µl) into one eye. We have recently demonstrated that CTB yields complete filling of retinofugal fibers (Angelucci et al., 1996), and as such is more suitable than WGA-HRP for revealing details of axon morphology.

Adult animals were anesthetized with ketamine and xylazine and an anesthetic ophthalmic solution was applied to the conjunctiva. The lateral aspect of the sclera was punctured, and the tracers were injected into the vitreal chamber with a 10-µl Hamilton microsyringe. Survival times of 2 and 4 days were allowed for the WGA-HRP- and CTB-injected animals, respectively. Fixation, sectioning, and processing of WGA-HRP material was performed as described above. Animals injected with CTB were perfused with saline followed by 4% paraformaldehyde, after which the brains were post-fixed in the same fixative overnight and cut at 40 µm in the coronal or horizontal plane. CTB was then revealed immunohistochemically according to the protocol of Angelucci et al. (1996). In all cases, every second brain section was processed for TMB or CTB, depending on the type of tracer injected, and counterstained with thionin. Adjacent brainstem and thalamic sections were stained for cytochrome oxidase.

Data analysis

Microscopic analysis of CTB labeled sections was carried out under brightfield and darkfield optics, whereas TMB stained sections were analyzed under darkfield and polarized light.

Inputs to the MGN. For every case that received injections of WGA-HRP/free HRP in the MGN (n = 5), retrogradely labeled cell bodies and fibers were examined on an entire series of 50-µm-thick brain sections, one every four sections (150-µm interval), and drawn by camera lucida at a total magnification of 375×. Although thionin counterstain allowed delineation of most nuclei and fiber tracts directly on the TMB material, cytoarchitectonic boundaries were further identified on adjacent Nissl and cytochrome oxidase stained sections. In one normal and three lesioned animals, labeled cells were counted on the reconstructed series of sections.

Extent of the neonatal lesions. For each case that received neonatal brain lesions, histological analysis of the extent of the lesions was performed at adulthood on Nissl and cytochrome oxidase stained sections. Because no published atlas of the ferret brain is currently available, brainstem and thalamic nuclei and fiber tracts were first identified in normal ferrets, by using as guidance an atlas of the cat brainstem (Berman, 1968) and thalamus (Berman and Jones, 1982). Because of the similarity between the two species, we have adopted the anatomical nomenclature and abbreviations of Berman (1968) and Berman and Jones (1982). In lesioned animals, identification of nuclei spared by the lesion as well as of partially lesioned brain structures did not prove to be a difficult task, because the overall cyto- and chemoarchitecture of the remaining brain tissue did not appear significantly altered when compared with that in normal animals. In this respect, the cytochrome oxidase material proved particularly useful, because the characteristic pattern of staining of brainstem nuclei and fiber tracts observed in normal animals, and on the unlesioned side of the brain, appeared essentially retained on the lesioned side (Fig. 2). In addition, the pattern of TMB staining of retinofugal projections was also useful to estimate the extent of lesion of the retinal targets.

Because neonatal lesions of a given brain structure often induce anterograde and/or retrograde transneuronal degeneration, damage to a primary structure might produce indirect atrophy of other nuclei. Indeed, in several instances, it was unclear whether, and to what extent, the reduction in size of a given nucleus was attributable to the primary neonatal lesion or to secondary degeneration. For example, because several auditory brainstem nuclei project to the IC as well as directly to the MGN, a primary lesion of IC might induce at least partial retrograde degeneration of some or all of these nuclei, thus resulting in more extensive deafferentation of the MGN than expected by the IC lesion alone. For this reason, for each lesioned case, we estimated not only the extent of the primary lesions but also the extent of lesion of all the brainstem and thalamic nuclei whose secondary or tertiary atrophy might have affected the interpretation of our results (see Figs. 5, 8, and Table 1). Because the main purpose of the present study was to correlate the extent of MGN deafferentation and of removal of retinal targets with the extent of novel retino-MGN projections, it was not necessary to ascertain whether the observed lesions were due to primary ablation or to secondary degeneration.

Lesion estimates were performed as follows. For each case, complete camera lucida reconstructions of the lesioned and unlesioned sides of the brainstem and thalamus were made from serial sections. Borders of nuclei were outlined on Nissl and cytochrome oxidase stained sections. For each lesioned structure, a lesion index (I_L) was then estimated as: I_L = 1- (existing structure), where (existing structure) was determined as the ratio between the total number of brain sections on the lesioned side still containing that structure and the total number of sections on a control in which the same structure was present. Wherever possible we used as control the unlesioned side of the brain in the same animal; however, for the few bilaterally lesioned animals, or for bilaterally lesioned structures, we used the mean value obtained from measurements in two normal animals (i.e., mean number of sections containing a given structure).

On the lesioned side of the brain, to score a brain structure as still present within, or absent from, a given brain section, we estimated its length and width, on both the lesioned and control sides, as the average of three measurements taken at regular intervals along its mediolateral and dorsoventral axes, and then scored the structure as "absent" from a brain section if either its mean length or its mean width measured less than 20% of its control length or width.

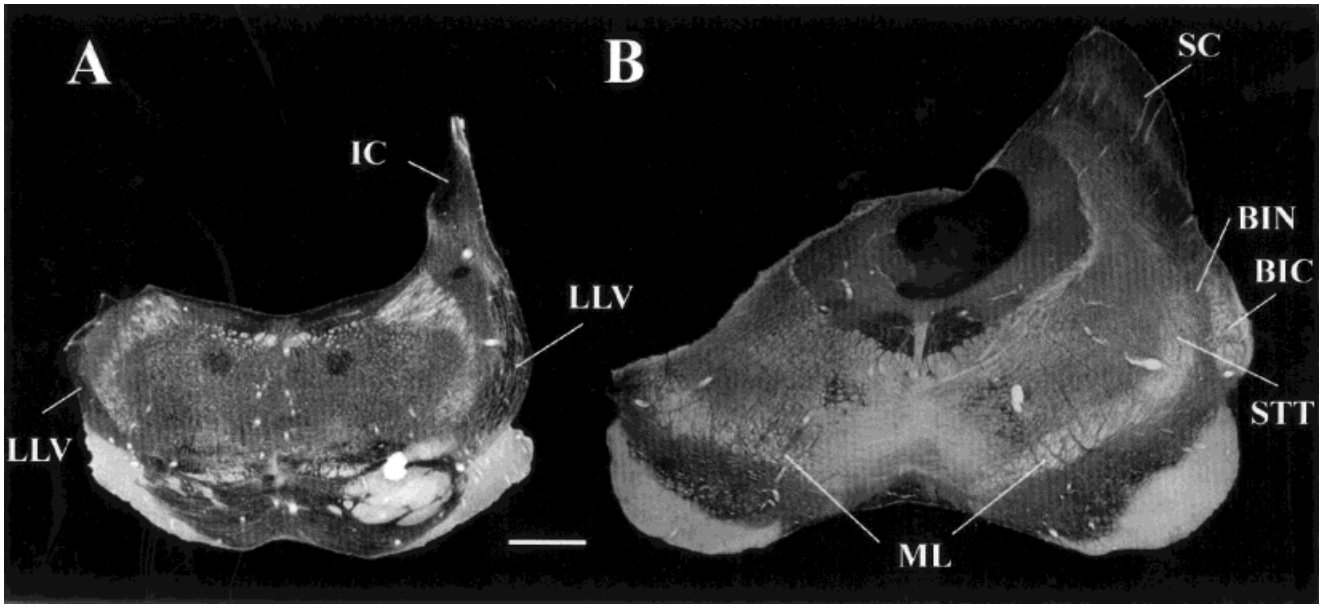

Fig. 2. Pattern of cytochrome oxidase staining of brainstem nuclei in unilaterally lesioned ferrets, as observed at adulthood. Coronal sections through the midbrain stained for cytochrome oxidase and shown under brightfield illumination. The type and extent of lesions is evident on the lesioned side of each section (left) when compared with the unlesioned side (right). Note that the chemoarchitectonic pattern of staining observed on the unlesioned side of the brain is essentially retained on the lesioned side. **A:** Coronal brainstem section taken approximately at the boundary between the pons and the caudal midbrain, showing, on the left, a lesion of the ventral nucleus of the lateral lemniscus (LLV). **B:** Coronal section through rostral midbrain, showing, on the left, lesions of the superior colliculus (SC), the brachium of the inferior colliculus (BIC), the nucleus of the BIC (BIN), and the spinothalamic tract (STT). For other abbreviations, see list. Dorsal is up. Digital images of partial brainstem sections were obtained by using a CCD camera (Sony DKC-5000) mounted onto a Leitz microscope, and connected to a computer (PC Dell M166s) equipped with a frame grabber, running a specialized software (Adobe Photoshop 3.0). With the same software, the resulting images were then cropped and mounted together to obtain the two composite images shown in the figure. Brightness and contrast of the separate portions of each image were matched, the background changed to black, and lettering and scale bar were added. Scale bar = 1 mm.

As defined above, I_L is essentially a measure of a reduction in the anteroposterior extent of a structure. However, because the neonatal lesions generally resulted at adulthood in a uniform reduction in size of the lesioned structure, i.e., along its three axes, I_L was effectively reflective of the overall lesion size. Thus, a lesion index of zero indicates complete sparing of a given brain structure, whereas a lesion index of 1 indicates 100% ablation.

In Figures 5, 8, to simplify the illustration of our data, after I_L was estimated for each structure of interest, lesions were grouped into three broader categories: (1) $<$50% (involving less than 50% of the structure), (2) $>$50% (involving more than 50% of the structure), (3) 100% (involving the whole structure).

Extent of retino-MGN projections. To allow for computerized calculations of the extent of retino-MGN projections, camera lucida drawings of a complete series of thionin-stained MGN sections and of WGA-HRP labeling were digitized. One in two sections throughout the rostrocaudal extent of MGN were analyzed for each case. We first calculated for each animal the total MGN area as the sum of all the pixels in all MGN sections multiplied by the pixel area. The total area of retino-MGN projections was then estimated as the sum of all the pixels with WGA-HRP label multiplied by the pixel area. Volumes in Table 1 were calculated as total MGN area, or total area of retino-MGN projections, multiplied by the distance between two adjacent sections. In Figure 8, the extent of retino-MGN projections is expressed as percent of the total MGN volume.

Axon caliber. Axon diameters of retinal ganglion cells projecting to the MGN were measured on two coronal and two horizontal CTB-stained MGN sections through the middle of the highest density of retinal innervation. Sections were taken from two different adult cases that had received extensive neonatal MGN deafferentation and complete ablation of the SC, but no lesion of visual cortex or of other retinal targets. The diameter of every axon entering the MGN, which had a clear axon trunk extending back to the optic tract, was measured in these four representative sections directly from the camera lucida, at a total magnification of 1500×. Because of the large number of filled axons, it was impossible to follow individual axons for long distances in the optic tract. Thus, measurements were taken every 50 μm along the axon trunk, from its most proximal end that could be clearly discerned (usually just proximal to its point of entrance into the MGN) to a distance of 150 μm within the nucleus. Measurements for each axon were then averaged.

RESULTS

Inputs to the MGN in normal adult ferrets

Injections of WGA-HRP and free HRP in the MGN of normal adult ferrets (n = 2) produced retrograde labeling of cell bodies in several brainstem auditory and non-

auditory nuclei. Ascending fibers to the MGN were also retrogradely labeled. The tracer deposits in both cases were of comparable size and were mostly confined to the MGN. In the TMB-stained sections, the HRP injection sites consisted of a core of dense reaction product, which appeared purple under darkfield illumination, surrounded by a lighter region, which had a golden appearance in darkfield. We considered the effective tracer uptake zone to correspond to the core-dense region. Camera lucida reconstructions of the injection site and the resulting labeling are shown for one such case at several thalamic and brainstem levels (Fig. 3). In both cases, the injection site extended from the caudal tip of the nucleus up to 0.8–1.0 mm rostrally and involved, at least in part, the ventral (MGv), the dorsal (MGd), and the medial (MGm) subdivisions of the MGN. However, in the case illustrated in Figure 3, the injection was located more medially that in the other case, thus including a larger portion of MGm and part of the suprageniculate nucleus (Sg). In the second case (not shown), the injection spared most of Sg.

As expected from similar studies in the cat, after unilateral injections of retrograde tracers in the MGN of normal adult ferrets, the majority of the label was found in the ipsilateral IC (Fig. 3), and involved all of its subdivisions, including the central and lateral nuclei, as well as the dorsal cortex. Cell counts indicated that approximately 80% of the total inputs to the MGN arose from the iIC. In addition, many retrogradely labeled cells (approximately 20% of the total) were also found in other auditory and non-auditory brainstem nuclei in both hemispheres (Fig. 3). The auditory nuclei that contained the largest number of retrogradely labeled cells, apart from the iIC, were the cIC, the ipsilateral dorsal nucleus of the lateral lemniscus (LLD), the contralateral and ipsilateral ventral nuclei of the lateral lemniscus (LLV), the ipsilateral nucleus of the brachium of the IC (BIN), and the contralateral and ipsilateral superior olivary complex (SO). Within the SO, labeled cells were found in both the lateral and medial nuclei (LSO and MSO, respectively). Moderate projections to the MGN arose also from the contralateral LLD and the ipsilateral and contralateral nucleus sagulum (SAG), whereas only a few labeled cells were observed in the ipsilateral nucleus of the trapezoid body (T). Non-specifically auditory afferents to the MGN arose primarily from the ipsilateral reticular thalamic nucleus (RTN; not shown) and, in the brainstem, from the contralateral and ipsilateral locus coeruleus (CAE), the dorsal (DR) and the linear central (LC) nuclei of the raphe, and the pontine and midbrain reticular formation, including the magnocellular (FTG), the lateral (FTL), the paralemniscal (FTP), and the central (FTC) tegmental fields on both sides. Fewer non-specifically auditory inputs to MGN arose from the marginal nucleus of the brachium conjunctivum (BCM), the dorsal tegmental nucleus of Gudden, and the ipsilateral SC (mainly from the deep layers, but in the case shown in Fig. 3, a few labeled cells were also observed in the superficial, retinorecipient layers of SC). A few labeled cells were also found in the periaqueductal gray (PAG), the cuneiform nucleus (Cu), and the contralateral vestibular nuclei (VN). In the case in which the injection site spared most of the Sg, and involved only the lateral part of MGm, no labeled cells were found in the VN, whereas only a few neurons were labeled in the deep layers of SC.

Retrograde HRP-labeling of fibers revealed the pathways followed by ascending brainstem afferents to the MGN (Fig. 3). Most retrogradely labeled fibers coursed caudorostrally in the ipsilateral BIC, and entered the MGN ventromedially. However, just caudal to MGN, at the level where the BIC forms a protrusion on the lateral aspect of the midbrain, many caudorostrally coursing fibers were located medial to BIC among the cell bodies of the BIN. At more caudal levels, some labeled axons ran ventral to BIC, in the lateral parts of the lateral lemniscus nuclei (LLV and LLD). Another group of axons entered the MGN dorsomedially. These fibers arose from the ipsilateral SC and the contralateral brainstem nuclei. It is noteworthy that the inputs ascending from the contralateral brainstem crossed the midline at the level of the SCC (Fig. 3).

Brainstem inputs to the MGN in neonatally operated ferrets

The above observations suggested that ablation of the BIC and/or iIC alone would spare many afferents to the auditory thalamus. To test this hypothesis, we examined the sources and pathways of inputs to the MGN in adult ferrets (n = 3) that had received different extents of MGN deafferentation at birth. Two of these animals received less extensive removal of MGN afferents than a third animal, and will be described first.

Inputs to the MGN in ferrets with less extensive MGN deafferentation. In two cases (F88–87 and F95–23; Figs. 4, 5), the MGN was partially deafferented at birth by complete ablation of the ipsilateral BIC and iIC, and minimal damage to the cIC. In case F95–23, to sever the inputs ascending from the contralateral brainstem, SCC was also ablated. In addition to partial deafferentation of the MGN, both animals also received partial removal of some normal retinal targets. This consisted of partial ablation of SC and of visual cortex (to reduce the size of the LGN) in case F88–87 (Fig. 4) and of complete ablation of SC alone in case F95–23. The extent of the neonatal lesions in both cases is reported in detail in Figure 5. The neonatal lesions performed in case F88–87 resembled those used in previous studies to induce retinal projections to the auditory thalamus (Frost, 1981,1982; Sur et al., 1988; Roe et al., 1993).

Large unilateral injections of retrograde tracers in the auditory thalami of these ferrets at adulthood indicated that, after unilateral BIC and IC removal, many brainstem afferents still innervate the MGN (Fig. 4). In case F88–87, the injection site extended about 1.6-mm anteriorly from the caudal pole of MGN and involved all its nuclear subdivisions, including Sg and the lateral part of the posterior group of thalamic nuclei (Po; Fig. 4). In case F95–23, the tracer deposit was smaller, and involved most of the caudal two thirds of MGd and MGv and the lateral parts of MGm and Sg. In both cases, label was found in the same brainstem nuclei, and, although regional variations in the number of labeled cells were observed, the total number of ipsilateral inputs to the MGN was comparable, and resembled that of ipsilateral extra-IC inputs to the MGN of normal animals (Fig. 5). Generally, on the side ipsilateral to the injection (see Fig. 4), labeled cells were more numerous in the lateral lemniscus nuclei (LLD and LLV), the BIN, and in the pontine and midbrain tegmental fields. Labeled cells were also observed in the deep layers of the remaining parts of SC, the ipsilateral CAE, SO, and SAG.

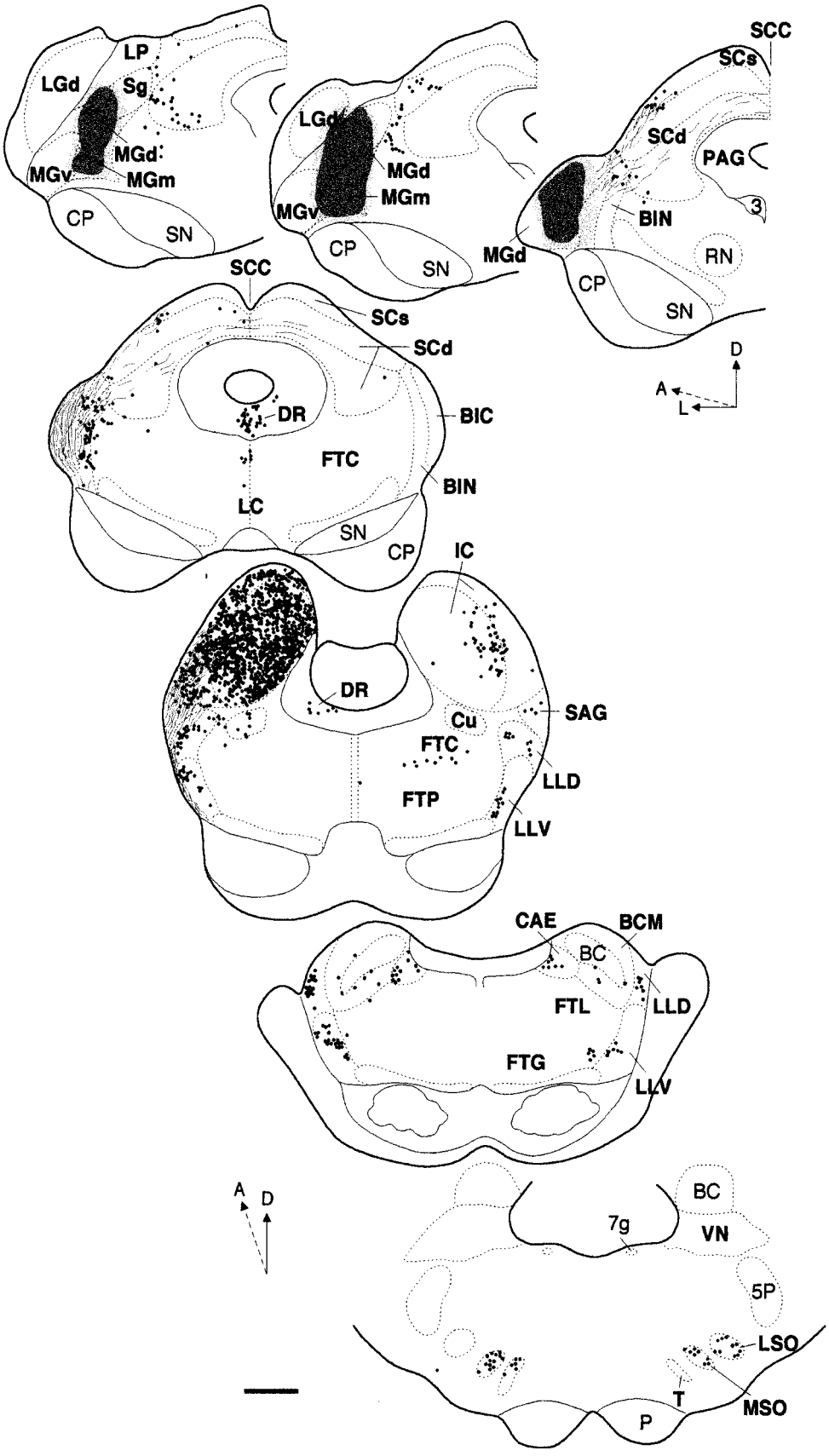

Fig. 3. Ascending brainstem inputs to the medial geniculate nucleus (MGN) in a normal adult ferret. Camera lucida drawings of coronal sections of the ferret caudal thalamus (top three sections) and brainstem (bottom four sections), from rostral (top) to caudal (bottom) levels. The core of the horseradish peroxidase injection site in the MGN, and the surrounding halo are represented in dark and light gray, respectively. Black dots represent retrogradely labeled cells; gray lines are retrogradely labeled fibers. In addition to inputs from the inferior colliculus (IC), the ferret MGN receives afferents from many other ipsilateral and contralateral brainstem nuclei. Many of these afferents follow extrabrachial pathways to reach the MGN. A, anterior; D, dorsal; L, lateral. For abbreviations, see list. Scale bar = 1 mm.

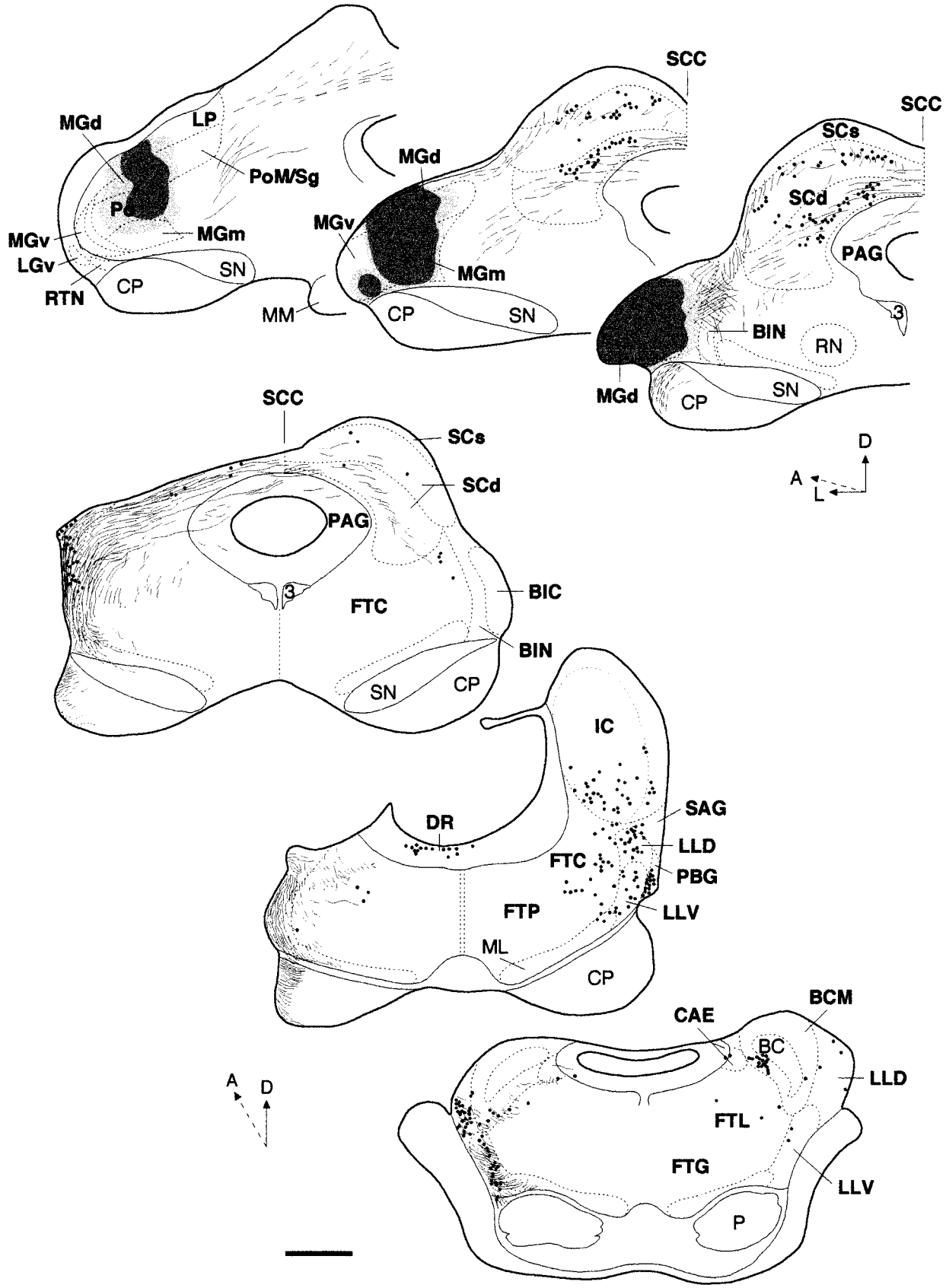

Fig. 4. Ascending brainstem inputs to the medial geniculate nucleus (MGN) after moderate MGN deafferentation in case F88–87. Camera lucida drawings of coronal sections of the caudal thalamus (top three sections) and brainstem (bottom three sections) of an adult ferret that received complete unilateral ablation of the brachium of the inferior colliculus (BIC) and the inferior colliculus (IC), and minimal damage to the contralateral IC. After BIC and IC removal, many inputs to the MGN are left intact. Many of these fibers follow novel pathways to reach the MGN (compare with Fig. 3; see Results section). A, anterior; D, dorsal; L, lateral. For abbreviations, see list. Scale bar = 1 mm.

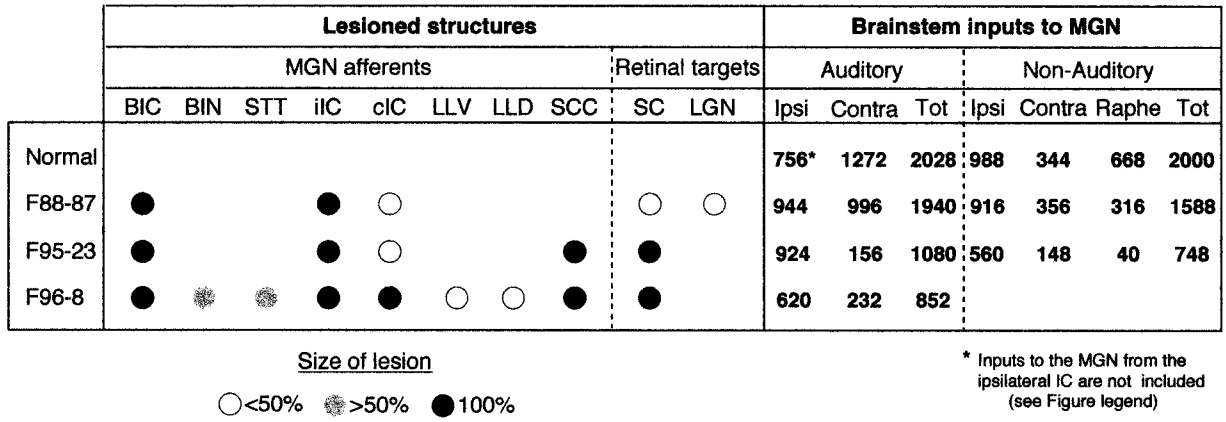

Fig. 5. Quantification of the inputs to the medial geniculate nucleus (MGN) arising from brainstem nuclei in normal and neonatally lesioned ferrets. Each row represents a different experimental case. The experiment number is indicated in the far left box. The middle box indicates the extent of neonatal lesion of MGN afferents and normal retinal targets. White, gray, and black circles represent the approximate percentage (indicated at the bottom left) of each neural structure that was absent in the adult animals (see Materials and Methods section). The right box shows the number of inputs to the MGN arising from auditory and non-auditory brainstem nuclei. Numbers indicate retrogradely labeled cells counted after unilateral tracer injections into the MGN. The auditory brainstem nuclei in which labeled neurons were counted were LLD, LLV, IC, BIN, SAG, PBG, SO, and T. Note that the number of labeled cells shown for the ipsilateral (ipsi) auditory brainstem nuclei in the normal animal (asterisk) does not include cells labeled in the ipsilateral inferior colliculus (IC). Approximately 80% (i.e., 15,488 neurons) of the labeled neurons were found in the ipsilateral IC in this case. The non-specifically auditory brainstem nuclei in which neurons were counted were CAE, the pontine and midbrain reticular formation (FTC, FTG, FTL, and FTP), BCM, the dorsal tegmental nucleus of Gudden, SC, PAG, Cu, and the raphe nuclei (DR and LC). Non-auditory brainstem nuclei in case F98–6 contained a larger number of labeled cells than the other cases due to spread of tracer (see text for details); these cells were not counted. Contra and Ipsi, number of labeled cells in the contralateral and ipsilateral nuclei, respectively; Tot, total number of labeled cells; Raphe, number of labeled cells in the raphe nuclei; BIC, brachium of the inferior colliculus; BIN, nucleus of the BIC; cIC, contralateral inferior colliculus; iIC, ipsilateral inferior colliculus; LGN, lateral geniculate nucleus; LLD, dorsal nucleus of the lateral lemniscus; LLV, ventral nucleus of the lateral lemniscus; SC, superior colliculus; SCC, commissure of the SC; STT, spinothalamic tract.

Whereas the amount of ipsilateral inputs to the MGN was similar in case F88–87 and F95–23, cell counts indicated that the number of labeled cells in brainstem nuclei contralateral to the injected MGN was significantly different in the two cases (Fig. 5). In case F88–87, which had received complete neonatal ablation of the ipsilateral BIC and iIC, and minimal damage to the cIC, the total number of contralateral labeled cells did not differ significantly from that observed in normal animals (Fig. 5). By contrast, four times as many contralateral labeled neurons were observed in this case than in case F95–23 (Fig. 5) in which the SCC had also been ablated. This reduction in the number of contralateral MGN inputs in case F95–23 was likely due to lesioning of SCC, because, as shown in normal ferrets, MGN inputs from the contralateral brainstem cross the midline at this level (Fig. 3). Although in case F88–87 most of the contralateral inputs to the MGN arose from both auditory and non-auditory brainstem nuclei (Fig. 4), in case F95–23 the remaining contralateral inputs arose mainly from the pontine and mesencephalic tegmental fields, and only few cells were found in auditory nuclei, including LLD, LLV and SO.

Figure 4 shows the pathways followed by ascending fibers to the MGN after unilateral lesions of BIC and IC. In coronal sections of caudal midbrain, retrogradely labeled fibers were observed in the lateral aspect of the mesencephalon, where they coursed caudorostrally mainly in the lateral lemniscus nuclei (LLV and LLD; Fig. 4, bottom two sections), but also in the lateral part of the midbrain tegmentum. In more rostral parts of the midbrain, at SC levels just caudal to the thalamus, although the BIC was clearly absent, a bundle of intensely stained fibers was observed in a region just medial to the site of the lesion. These fibers invaded the BIN and, medial to this, the spinothalamic tract. Ascending fibers from the contralateral brainstem crossed the brain midline in the SCC, as in normal controls, traversed the deep layers of the ipsilateral SC, and either joined the fiber bundle in the BIN, caudal to the MGN, or entered the dorsomedial aspect of the MGN more rostrally. Because in case F88–87 the caudal part of SC had been ablated at birth, at this level SCC was reduced in size. Fibers were observed to cross the midline in the remaining parts of SCC, but, different from normal animals, also at more ventral positions, in the PAG.

The above observations indicated that after unilateral removal of BIC and IC alone, many afferents still innervated the MGN. Some of these afferents were fibers that normally do not course in the BIC, and thus were spared by the neonatal BIC lesion. However, other afferents consisted of fibers that, in response to the neonatal injury, followed novel trajectories to reach the MGN (compare fiber pathways in Figs. 3 and 4).

Inputs to the MGN in ferrets with extensive MGN deafferentation. Injections of retrograde tracers in the MGN of a third animal (F96–8; Figs. 5, 6) that had received a large neonatal bilateral transection of the lateral mesencephalon (including BIC and regions ventral to BIC, most of BIN, and the rostral parts of the lateral lemniscus nuclei), along with complete bilateral ablation of IC and SC, resulted in a marked reduction in the number of retrogradely labeled cells in the ipsilateral and contralateral auditory brainstem nuclei (Fig. 5). The injection site involved most of the anteroposterior extent of the MGN, was centered in MGv, but also included Po and the lateral aspect of MGd and MGm. In addition, rostrally, the

TABLE 1. Quantitative Data on the Extent of MGN Deafferentation, Extent of Novel Retino-MGN Projections, and MGN Size in Lesioned Ferrets[1]

Animal	BIC Lesion Index	IC Lesion Index	SC Lesion Index	LGN Lesion Index	MGN volume (mm^3)	Retino-MGN projections (mm^3)
F93-50	0.2	0.5	1	0.75	1.2	0.003
F93-70	0.57	0.47	0.1	0.15	2.4	0.04
F93-67	0.57	0.45	1	0.2	2.3	0.04
F94-97	1	1	1	0	2.5	0.07
F95-75	1	1	1	0	2.6	0.13
F93-138	1	1	1	0.6	1.5	0.09
F93-111	1	1	1	0.72	2.36	0.09
F93-158	1	1	1	0	1.6	0.06

[1]BIC, brachium of the inferior colliculus; IC, inferior colliculus; LGN, lateral geniculate nucleus; MGN, medial geniculate nucleus; SC, superior colliculus. For a description of how the Lesion Index was calculated, see the Materials and Methods section.

tracer deposit encroached upon small adjacent portions of the lateral posterior thalamic nucleus (LP), RTN, and LGN (Fig. 6). A large number of retrogradely labeled cells was found in non-specifically auditory brainstem nuclei, including the pontine and mesencephalic tegmental fields, the raphe nuclei, the CAE, and the BCM (Fig. 6). The larger number of labeled cells observed in these nuclei, compared with other lesioned (Fig. 4) and normal (Fig. 3) cases, could be attributed to the spread of tracer to the RTN and LP. However, the number of inputs from the auditory brainstem nuclei was markedly reduced compared to normal controls and cases with less extensive deafferentation of the MGN (Fig. 5). Labeled cells were observed mainly in the remaining parts of LLD, LLV, and ipsilateral BIN, and only a few cells were labeled in the SO.

Overall, the above observations indicated that significant deafferentation of the MGN was achieved by the following combination of neonatal lesions: (1) large mesencephalic transection at midcollicular level, including BIC, but also parts of the lateral tegmentum medial and ventral to it (the medial extension of this cut severed at least part of the BIN and seemed to prevent growth of fibers around the site of injury, whereas extension of the lesion ventral to BIC caused severance of extra-BIC fibers that normally run in the ventrolateral aspect of the mesencephalon); (2) complete bilateral ablation of the IC, the main source of inputs to the MGN; and (3) complete ablation of the commissure of the SC, to sever afferents to MGN arising from contralateral auditory brainstem nuclei.

Extent of the novel retino-MGN projection in relation to different types of neonatal lesions

Next, we tested whether the extent of MGN deafferentation correlates with the amount of anomalous retinal projections to the MGN (Fig. 1B–C), and whether extensive removal of normal retinal targets further increases the quantity of this projection (Fig. 1D). In different newborn ferrets (n = 15), varying degrees of MGN deafferentation were combined with varying degrees of lesion of normal retinal targets (including SC, LGN, and PT). Bilateral intraocular injections of WGA-HRP were made in these animals at adulthood to reveal the extent of the ectopic projections. An example of WGA-HRP labeled retino-MGN projections is shown in Figure 7.

The extent of the lesions and the resulting extent of retino-MGN projections were quantified for nine representative cases (see Materials and Methods section). Even though we used a highly standardized surgical protocol to produce neonatal lesions, in the adult animals we observed an unavoidable degree of variability in the final extent of the lesions. It was, thus, necessary to report our observations for each individual case separately (Fig. 8).

In Figure 8, to facilitate interpretation as well as illustration of the data, a lesion index (I_L) was first estimated for each lesioned structure (as described in the Materials and Methods section), after which lesions were grouped into three broader categories: lesions involving less than 50%, more than 50%, or 100% of a brain structure. Lesion indices for BIC and IC, the main sources of MGN inputs, and for SC and LGN, the main retinal targets, are reported for each case in Table 1.

The extent of the novel retino-MGN projections resulting from different combinations of neonatal lesions is expressed in Figure 8 as percentage of the total MGN volume, and is grouped into two broad categories: cases in which less than 2% of MGN was innervated by retinal axons, and cases with more significant retinal innervation of MGN (more than 2% and up to 6%). Note that our estimates of the percentage volume of the MGN invaded by retinal fibers are percent of the entire MGN, including all of its subdivisions, i.e., MGv, MGd, MGm, Po, Sg, and the pars lateralis of the ventral division of MGN (vl; Figs. 9, 10). Actual volumes of retino-MGN projections are reported for each case in Table 1. Because absolute volumes of retino-MGN projections are affected by interanimal variability (mainly due to brain size and sex differences), we thought it more appropriate to express the amount of novel retinal projections as percentage of MGN volume.

The data illustrated in Figure 8 indicate that the animals with the most severe early damage to the ascending auditory pathway showed the most extensive retinal projection to the MGN. By contrast, the extent of removal of normal retinal targets did not seem to affect the amount of retino-MGN projections.

Figure 9 shows an example of retinal afferents to the auditory thalamus, after >50% removal of BIC (I_L= 0.57), <50% ablation of the iIC (I_L= 0.47%), and <50% ablation of LLV, and LLD (I_L= 0.35 and 0.2, respectively). The percentage of MGN innervated by retinal fibers in this case (1.67%, F93–70) was comparable to that observed in another animal (1.74%, F93–67) that received a similar extent of MGN deafferentation (BIC I_L = 0.57; IC I_L = 0.45; SCC I_L = 0.6), but more extensive removal of retinal targets (see Fig. 8 and Table 1).

Figure 10 shows an example of retino-MGN projections in an animal (F95–75) that received extensive bilateral MGN deafferentation (I_L for BIC, iIC, cIC, and SCC = 1; BIN I_L = 0.8; I_L for LLV and LLD = 0.3) along with complete bilateral removal of SC (I_L = 1), but no lesion of LGN or PT. The amount of retino-MGN projections in this case (5%), was significantly enhanced compared to that in animals (0.25% in F93–50, 1.74% in F93–67) with less severe removal of MGN inputs but more extensive ablation of normal retinal targets (compare case F95–75 with cases F93–67 and F93–50 in Fig. 8 and Table 1). No significant difference in the percentage of MGN innervated by retinal projections was observed in case F95–75, compared to that in other cases (3.8% in F93–111, 6% in F93–138, 3.75% in F93–158) with similar extent of MGN deafferen-

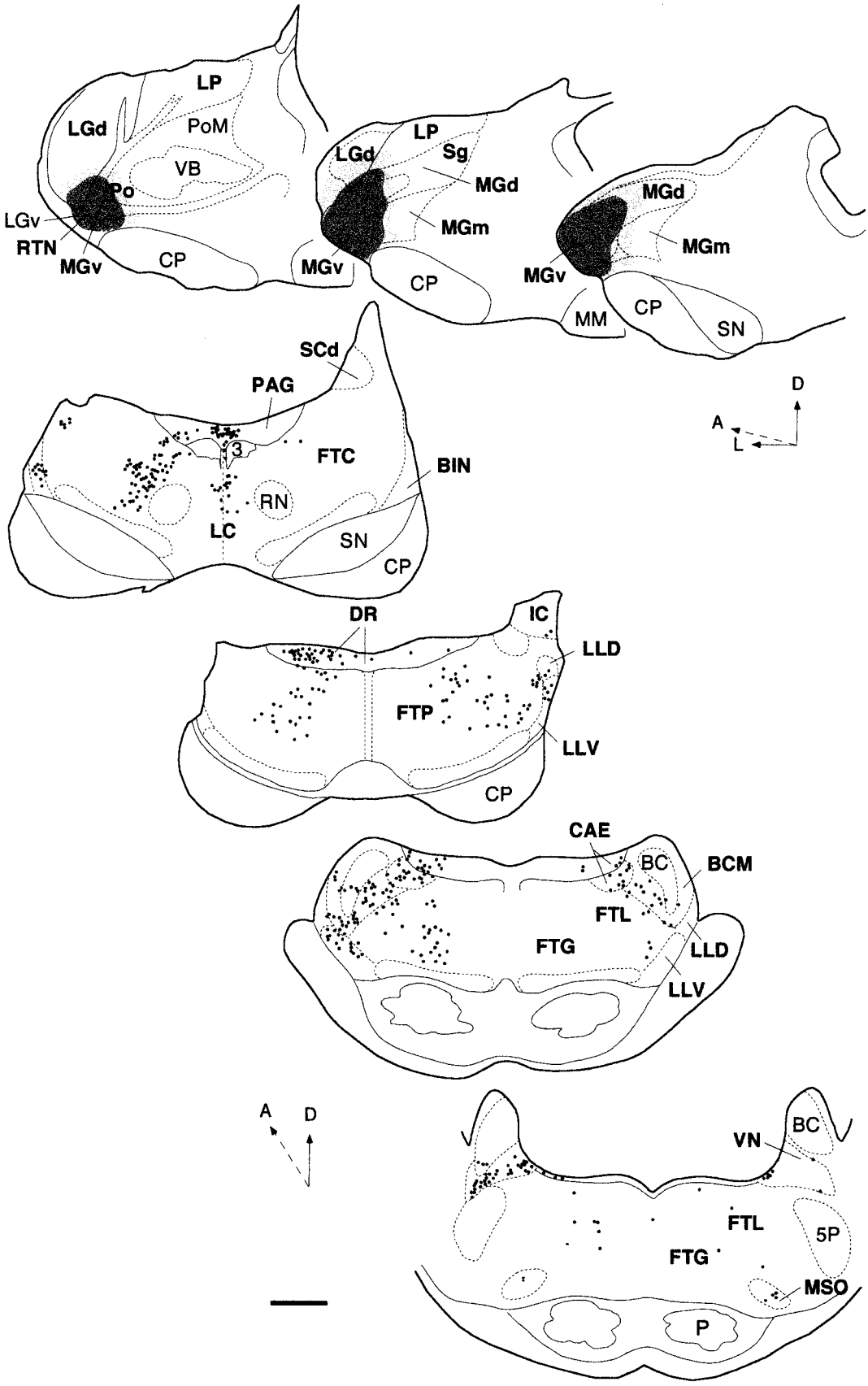

Fig. 6. Ascending brainstem inputs to the medial geniculate nucleus (MGN) after extensive neonatal MGN deafferentation in case F96–8. Camera lucida drawings of coronal sections of the caudal thalamus (top three sections) and brainstem (bottom four sections) of an adult ferret that received extensive neonatal bilateral lesions of the lateral mesencephalon and complete bilateral ablation of the superior and inferior colliculi. Inputs to the MGN from auditory brainstem nuclei are markedly reduced compared to normal controls (compare with Fig. 3) and cases with less extensive MGN deafferentation (compare with Fig. 4). A, anterior; D, dorsal; L, lateral. For abbreviations, see list. Scale bar = 1 mm.

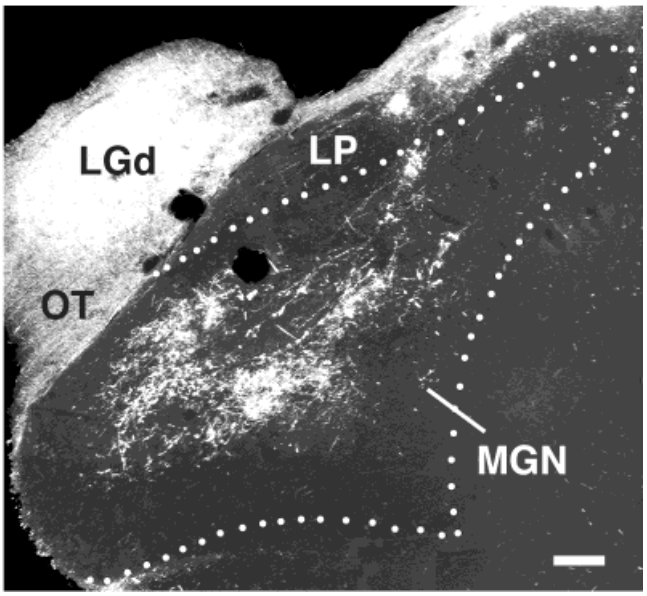

Fig. 7. Novel retinal projections to the medial geniculate nucleus (MGN) labeled after intraocular injection of wheat germ agglutinin conjugated to horseradish peroxidase. Coronal section through the MGN, shown under darkfield illumination, in an adult ferret that received extensive neonatal deafferentation of the MGN, and complete ablation of the superior colliculus. The dotted line shows the outer border of the MGN. Dorsal is up, and medial is to the right. Digital images of the MGN section were obtained by using a CCD camera (Sony XC-77CE) mounted onto a Zeiss microscope, and connected to a Power Macintosh (9500/120) equipped with a frame grabber, running a specialized software (Image 1.44). The resulting PICT files then were imported onto Adobe Photoshop 4.0, cropped, and mounted together to obtain a composite image. Brightness and contrast of the separate portions of the image were matched, and lettering, symbols, and scale bar were added using the same software. For abbreviations, see list. Scale bar = 200 μm.

tation but more extensive removal of retinal targets (see Fig. 8 and Table 1).

Thus, the data in Figure 8 indicate that the amount of anomalous retinal projections correlated well with the extent of MGN deafferentation, but not with the extent of removal of normal retinal targets. However, it was important to ascertain that an increased percentage of MGN innervation by retinal afferents, in cases with more extensive MGN deafferentation, was in fact due to an actual increase in the amount of retinal projections rather than to a reduction in MGN volume caused by deafferentation.

Statistical analysis revealed that the mean MGN volume (1.97 mm^3, SEM = 0.38, n = 3) in cases with less extensive MGN deafferentation (F93–50, F93–70, and F93–67 in Fig. 8 and Table 1), and the mean MGN volume (2.11 mm^3, SEM = 0.23, n = 5) in cases with more extensive MGN deafferentation (cases F94–97 to F93–158 in Fig. 8 and Table 1) were not significantly different (P = 0.74; Student's t-test). By contrast, the mean volume of retino-MGN projections in cases with more extensive MGN deafferentation (0.088 mm^3, SEM = 0.012, n = 5) was significantly greater (P = 0.016) than that in cases with less extensive MGN deafferentation (0.027 mm^3, SEM = 0.012, n= 3). Furthermore, whereas lesion indices (I_L) for BIC or IC, the two main sources of MGN inputs, were positively and significantly correlated with the volume of retino-MGN projections (r = 0.855, $P < 0.01$, for BIC; r = 0.791, P = 0.019, for IC; Pearson's correlation), they did not significantly correlate with the volume of the MGN (r = 0.375, P = 0.359, for BIC; r = 0.111, P = 0.793, for IC). Scatter plots and best fit lines relating retino-MGN projections and MGN volumes to the BIC lesion are shown in Figure 11A,B.

Overall, the above analysis indicated that the increased percentage of MGN innervation by retinal fibers, observed in cases with more extensive MGN deafferentation, was not due to a reduction in the volume of the MGN, but rather to an actual increase in the amount of the retinal projection.

By contrast, no significant correlation was found between lesion indices for SC or LGN, the two main retinal targets, and the volume of retino-MGN projections (r = 0.283, P = 0.49, for SC; r = −0.237, P = 0.57, for LGN), or the volume of the MGN (r = −0.258, P = 0.53, for SC; r = −0.529, P = 0.177, for LGN). Scatter plots of data related to the LGN lesion are shown in Figure 11C,D.

Deafferentation of the auditory thalamus not only affected the quantity of anomalous retinal projections, but as previously reported (Roe et al., 1993), also appeared to be necessary to induce sprouting of retinal axons in the MGN. Indeed, regardless of the extent of removal of retinal targets, little or no ectopic projections were found when the BIC was only minimally damaged or not lesioned (see for example case F93–50; Fig. 8 and Table 1). The latter results also indicated that ablation of SC, LGN, and/or PT by itself is not sufficient to generate novel retinal projections. Moreover, even when combined with deafferentation of the MGN, removal of the LGN and/or PT did not affect the quantity of the novel projection (see cases F94–97 and F95–75 in Fig. 8). However, it was more difficult to determine whether deafferentation of the MGN is by itself sufficient to induce retino-MGN projections, or whether at least some removal of the SC is also required. The main reason is that it was technically difficult to perform a large lateral transection of the midbrain without producing serious damage to the overlying SC. In addition, SC is not only a retinal target (superficial layers), but also a source (deep layers) of, and a pathway (intercollicular commissure) for, afferents to the MGN. The technical difficulty of ablating the deep collicular layers and the intercollicular commissure while preserving the superficial retinorecipient layers of SC, prevented us from directly testing whether MGN deafferentation alone is sufficient to induce maximal retinal innervation of MGN. Nevertheless, comparison between cases F93–70 and F93–67 (Fig. 8 and Table 1), which received a similar extent of MGN deafferentation and similar damage to the LGN, but significantly different extents of SC lesion, indicated that the extent of SC removal does not significantly correlate with the extent of retino-MGN projections. Unfortunately, to minimize the damage to the SC in case F93–70, we could not perform an extensive deafferentation of the MGN.

In one extreme case (F93–69; Fig. 8), complete ablation of SC and LGN, along with extensive damage to PT, resulted in marked retrograde atrophy of the optic tract (Fig. 12A) and no retinal projections to the MGN (Fig. 12B), even though BIC and SCC had been completely ablated. Intense labeling of the few remaining retinal targets (nuclei and fiber tracts of the accessory optic system and remnants of PT) on the side of the lesion (Fig. 12B), as well as on the contralateral, unlesioned side (right

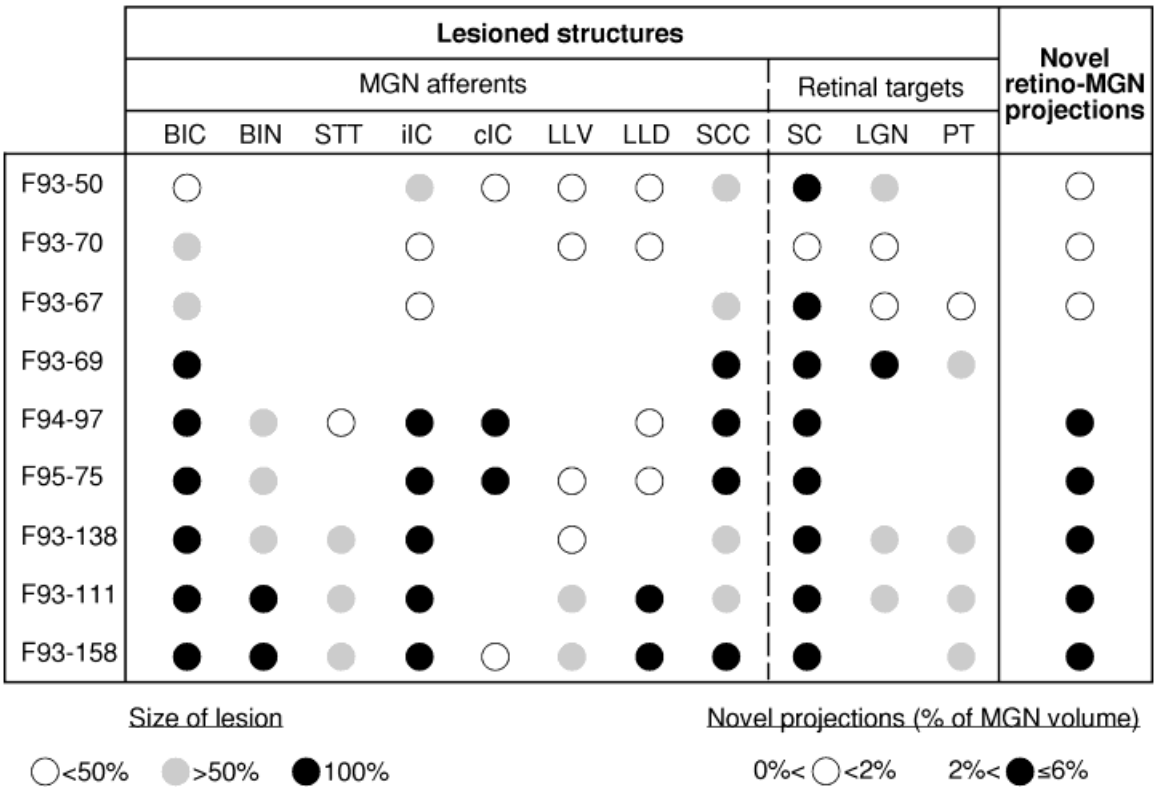

Fig. 8. Factors affecting the quantity of anomalous retinal projections to the medial geniculate nucleus (MGN). Each row represents a different experimental case. The experiment number is indicated in the far left box. The middle box indicates the extent of neonatal lesion of MGN afferents (left) and normal retinal targets (right). The extent of lesion is represented as white, gray, and black circles as in Fig. 5. The resulting amount of retino-MGN projections obtained in each lesioned case is indicated in the far right box. White and black circles in the far right box represent the percentage of MGN volume innervated by retinal fibers (indicated at the bottom right). Note that the amount of novel projections to the MGN correlates well with the extent of removal of MGN afferents, but not with the extent of removal of normal retinal targets (see Results section). BIC, brachium of the inferior colliculus; BIN, nucleus of the BIC; cIC, contralateral inferior colliculus; iIC, ipsilateral inferior colliculus; LGN, lateral geniculate nucleus; LLD, dorsal nucleus of the lateral lemniscus; LLV, ventral nucleus of the lateral lemniscus; PT, pretectal nuclei; SC, superior colliculus; SCC, commissure of the SC; STT, spinothalamic tract.

OT in Fig. 12A), indicated that the tracer had been effectively transported by retinal cells. Thus, the presence of at least some normal retinal targets seems to be necessary for retinal fibers to innervate the MGN.

Novel non-retinal inputs to the MGN following early extensive removal of normal auditory afferents

Even after extensive removal of ascending auditory inputs to the MGN, retinal projections innervated no more than 6% of the total MGN volume (Fig. 8 and Table 1). As previously reported (Angelucci et al., 1997), retinal axons were consistently found to "prefer" the rostral MGN. Our estimates indicated that approximately 10% of the rostral half of the nucleus receives retinal afferents.

Despite extensive removal of auditory afferents and only partial innervation by retinal fibers, the MGN in lesioned animals usually appeared normal in size and morphology when compared with the MGN in normal animals. This striking observation suggested that in addition to retinal inputs and remnants of brainstem inputs spared by the neonatal lesion (see above), other input types also innervated the MGN. To test this hypothesis, retrograde tracers were injected into the MGN of two rewired ferrets (cases F95–23 and F96–8 described above; Fig. 5) that had received moderate and extensive MGN deafferentation, respectively, along with complete ablation of SC. The lower brainstem as well as the cervical spinal cord were examined for retrograde labeling. The resulting labeling of cell bodies in both cases revealed that a variety of non-retinal afferent systems innervated the MGN. Remnants of normal auditory and non-specifically auditory brainstem afferents to the MGN observed in these cases have been described above (see also Fig. 6).

Novel non-retinal inputs to the MGN (Fig. 13) arose from the ipsilateral and contralateral dorsal column nuclei in the medulla, including both the gracile (GR) and cuneate (CUN) nuclei, the ipsilateral and contralateral spinal nucleus of the trigeminal nerve (5SP), the contralateral medial and lateral nuclei of the solitary tract (ST), and the contralateral dorsal horn of the cervical spinal cord (not shown; the thoracic and lumbar spinal cord were not analyzed). In addition, in case F96–8, but not in case F95–23, many more retrogradely labeled cells were observed in the ipsilateral and contralateral VN (Fig. 6) compared with normal controls (Fig. 3). Table 2 summarizes the quantitative data on the novel, non-retinal inputs to the MGN in lesioned animals compared with normal controls. Importantly, similar to the novel retinal projection, the amount of novel non-retinal inputs to the MGN

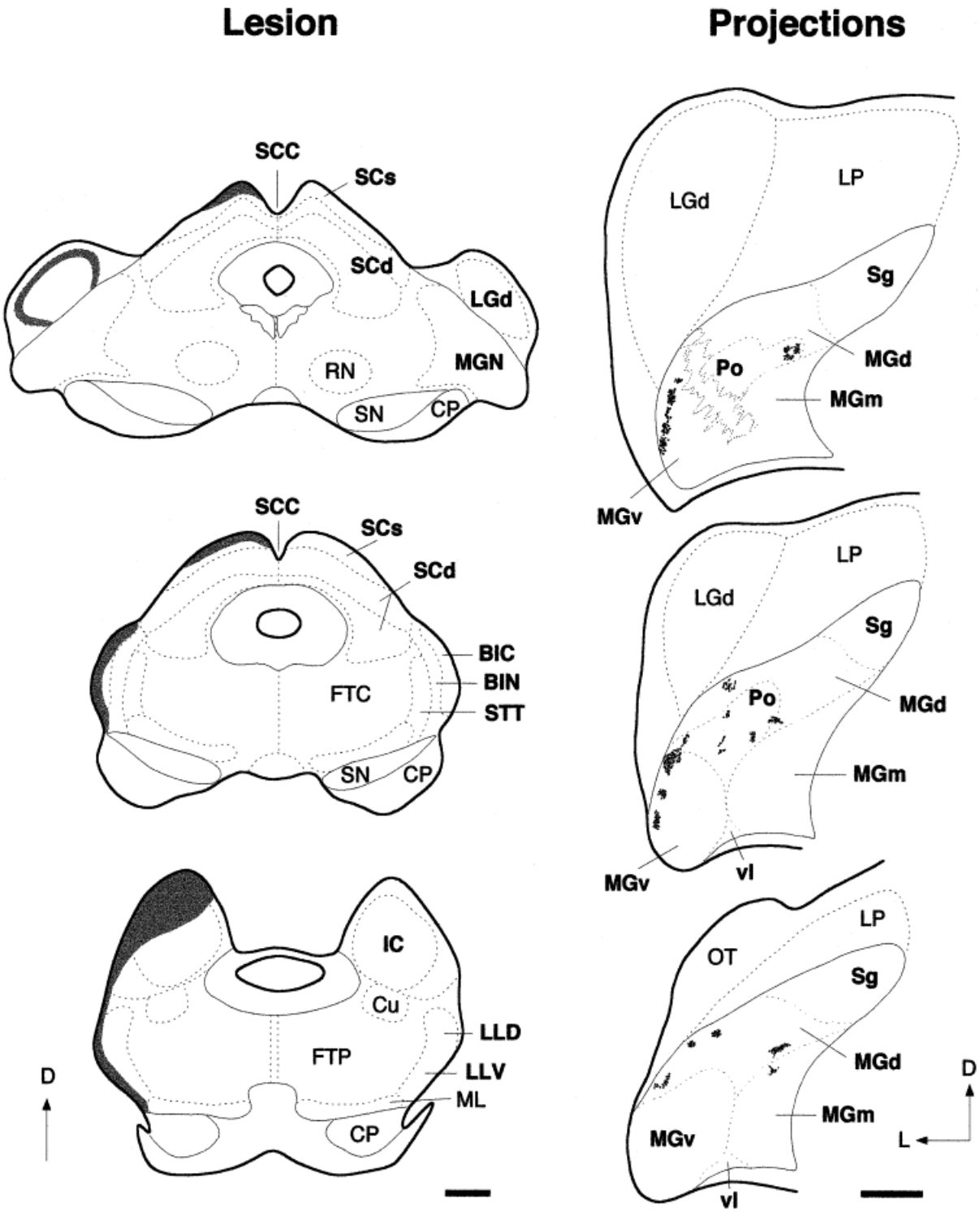

Fig. 9. Novel retinal projections to the medial geniculate nucleus (MGN) after moderate MGN deafferentation (case F93–70; see Fig. 8). Left: Extent of the lesions. Line drawings of coronal sections of a ferret standard thalamus and brainstem from rostral (top) to caudal (bottom) levels. Gray areas indicate the approximate extent of the lesion performed at birth estimated by comparison with the contralateral, unlesioned side (see Materials and Methods section). Right: Retino-MGN projections. Camera lucida drawings of coronal sections of rostral MGN, from rostral (top) to more caudal (bottom) levels, showing the novel retinal projection obtained as a result of the neonatal lesions shown on the left. Sections were taken at the MGN level of maximal retinal label. D, dorsal; L, lateral. For abbreviations, see list. Scale bars = 1 mm (left), 500 μm (right).

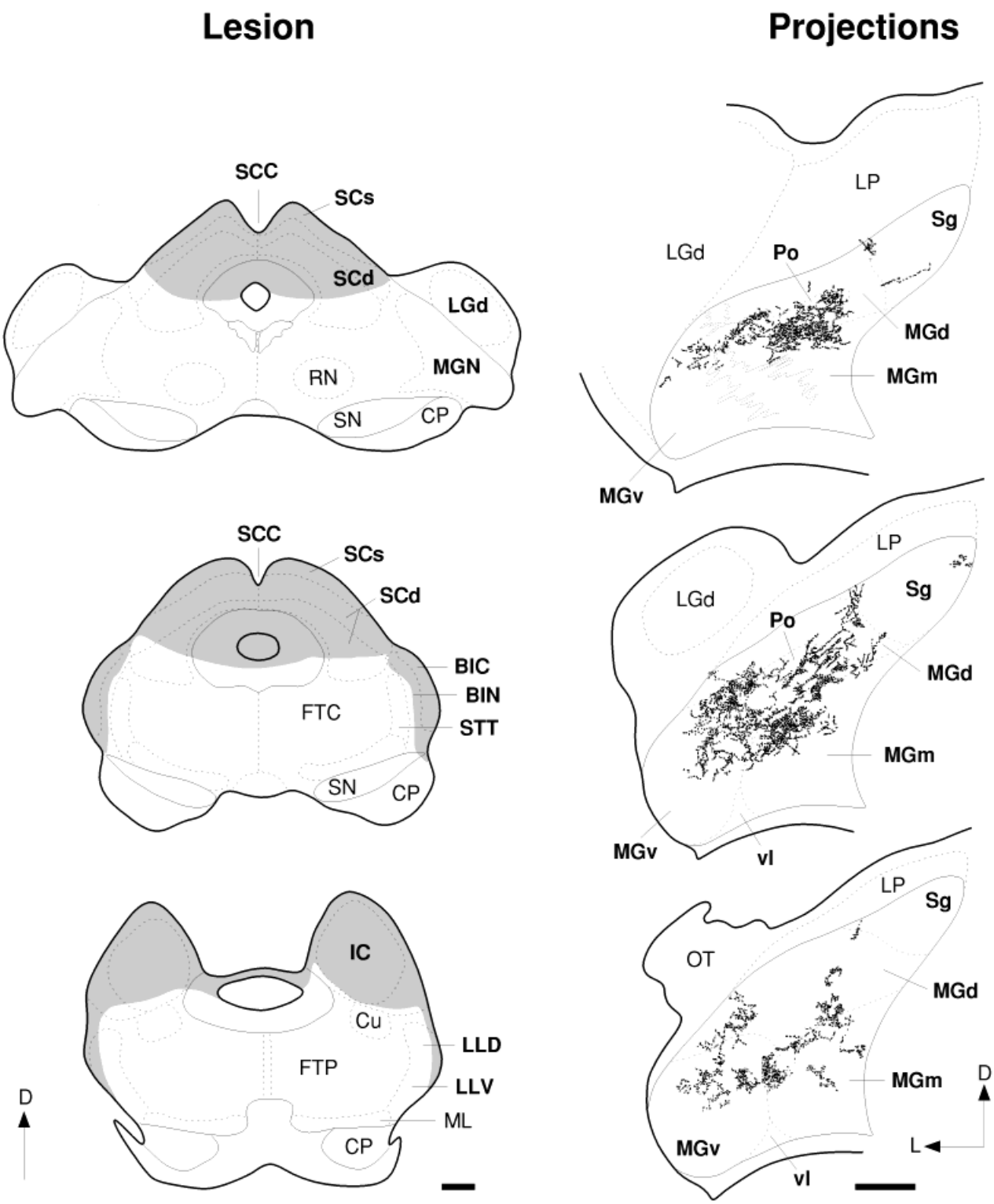

Fig. 10. Novel retinal projections to the medial geniculate nucleus (MGN) after extensive MGN deafferentation (case F95–75; see Fig. 8). Left: Extent of the lesions. Line drawings of coronal sections of a ferret standard thalamus and brainstem from rostral (top) to caudal (bottom) levels. Right: Retino-MGN projections. Camera lucida drawings of coronal sections of the MGN, from rostral (top) to caudal (bottom) levels, showing the novel retinal projection obtained as a result of the neonatal lesions shown on the left. Sections were taken at the MGN level of maximal retinal label. D, dorsal; L, lateral. For abbreviations, see list. Scale bars = 1 mm (left), 500 μm (right).

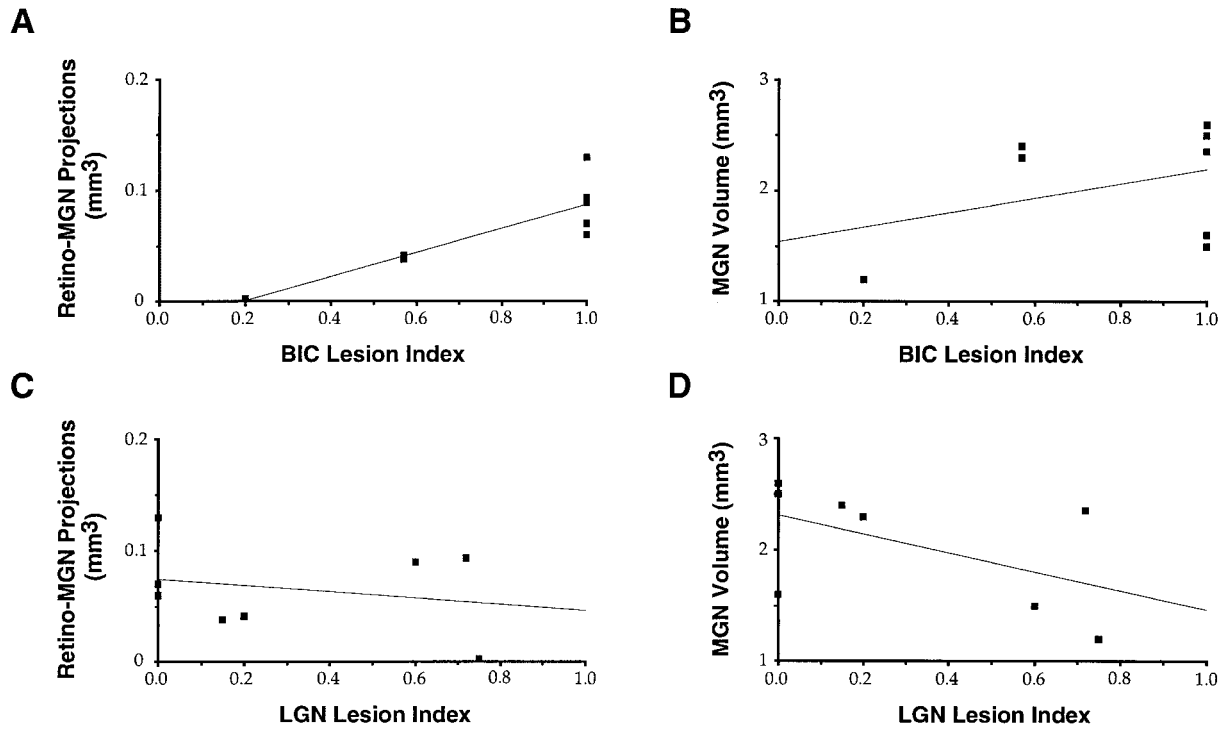

Fig. 11. Scatter plots and lines of best fit of various correlations: **A:** Volume of retino-MGN projections versus extent of lesion of the brachium of the inferior colliculus (BIC) (Lesion Index; see Materials and Methods section). **B:** MGN volume versus extent of BIC lesion. **C:** Volume of retino-MGN projections versus extent of lesion of the lateral geniculate nucleus (LGN). **D:** MGN volume versus extent of LGN lesion. For abbreviations, see list.

also seems to correlate well with the extent of removal of its normal afferents. Case F96–8, which received more extensive MGN deafferentation than case F95–23 (see Fig. 5), showed a significantly higher number of novel non-retinal afferents to the auditory thalamus (Table 2).

Axon caliber of retinal ganglion cells projecting to the MGN

Previous studies from this laboratory suggested that the novel retino-MGN projection arises from the W-class of retinal ganglion cells (Roe et al., 1993; Pallas et al., 1994). However, the previous lesion paradigm to redirect retinal projections to the auditory thalamus included ablation of the visual cortex, to induce retrograde degeneration of the LGN. The present observation that retinal axons can be induced to innervate the MGN without lesioning visual cortex or LGN raised the question of which retinal cell types project to the MGN under the new paradigm.

Because the MGN is surrounded by normal retinal targets and fiber tracts, we found it difficult to deliver a large deposit of retrograde tracers that was exclusively confined to the MGN and did not involve, even minimally, any surrounding normal retinal structures. For this reason we did not use retrograde transport to identify retinal ganglion cells, but instead examined the axon caliber of retinal cells projecting to the MGN, labeled by eye injections of an anterograde tracer. For this purpose, intraocular injections of CTB were made in adult ferrets with early extensive deafferentation of the MGN and complete ablation of the SC, and the diameters of retino-MGN axons were measured (see Materials and Methods section). Data were then compared with previously published data on the caliber of retinal axons in the MGN of ferrets with visual cortical lesions (Pallas et al., 1994) and of X, Y, and W axons in the normal ferret LGN (Roe et al., 1989; Pallas et al., 1994).

In the present study, the diameters of retinal axons in the MGN were found to range between 0.2 and 3.6 μm (mean, 1.04 μm; SEM = 0.135; n = 44). These values overlap only in part with those reported for retino-MGN axons in ferrets with visual cortical lesions (range, 0.2–1.79 μm; mean, 0.74 μm; SEM = 0.07, n = 31; Pallas et al., 1994). Axon diameters were measured in similar fashion to Pallas et al. (1994): a series of measurements were taken at regular intervals along the axon trunk, from a location in the optic tract just proximal to the axon's point of entrance in the MGN, up to a defined distance within the nucleus, and then averaged (see Materials and Methods section). The mean diameters of the populations of retino-MGN axons differed significantly ($P < 0.05$, Student's t-test). The diameters of X axons (range, 1.4–2.0 μm; mean, 1.6 μm; Roe et al., 1989), Y axons (range, 2.0–3.7 μm; mean, 2.9 μm; Roe et al., 1989), and W axons (range, 0.2–1.59; mean, 0.78 μm, SEM = 0.09; Pallas et al., 1994) in the normal LGN overlap extensively with the diameters of retino-MGN axons found in the present study. However, because Roe et al. (1989) measured the caliber of retino-LGN axons in the optic tract, and because we cannot exclude the possibility that our axonal population included collateral branches of main axons, a direct comparison between the diameters of retino-MGN axons and those of retino-LGN axons cannot be made. Nevertheless, it is noteworthy that at least the thickest retino-MGN axons found in the present study had calibers that approximated

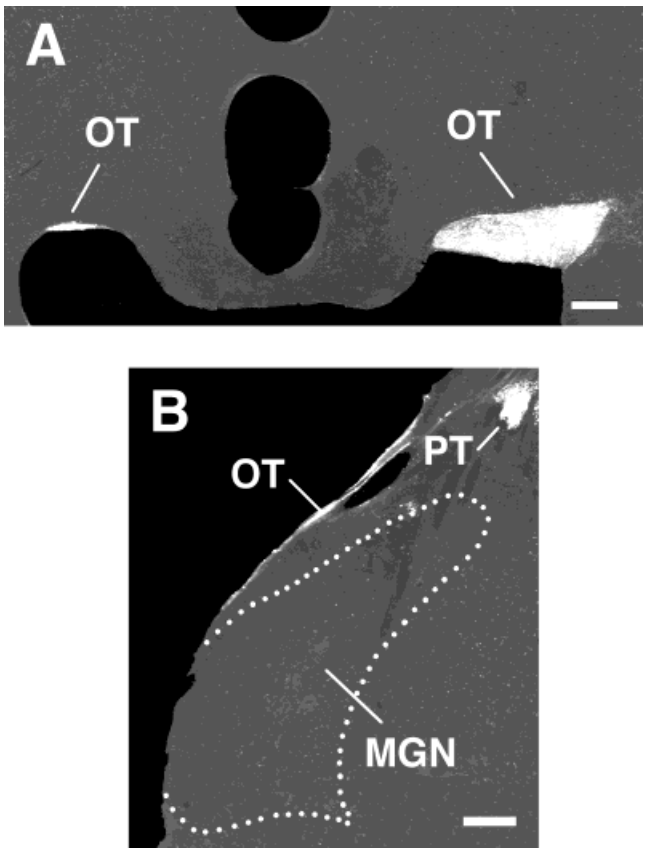

Fig. 12. **A:** Marked atrophy of the optic tract (OT) in case F93–69 (see Fig. 8), which received extensive unilateral lesion of the pretectal nuclei and complete unilateral ablation of the brachium of the inferior colliculus, the superior colliculus (SC), the commissure of SC, and the lateral geniculate nucleus. Retinofugal projections were labeled by bilateral intraocular injections of wheat germ agglutinin conjugated to horseradish peroxidase and viewed under darkfield illumination and polarized light. The atrophy of the optic tract (left in the figure) on the side of the neonatal lesions is evident when compared with the normal OT (right in the figure) on the unlesioned hemisphere. **B:** Lack of retinal projections to the medial geniculate nucleus (MGN) in case F93–69. Coronal section through the MGN, viewed under darkfield illumination and polarized light. Digital images of the brain sections were obtained and processed as described in the legend of Figure 7. The dotted line shows the outer border of the MGN. PT, pretectal nuclei. Scale bars = 500 μm in A, 300 μm in B.

those of the thickest Y axons in the normal ferret LGN, suggesting that the novel retino-MGN projection might now arise from more than one type of retinal ganglion cells.

DISCUSSION

We have shown that, in addition to inputs from the ipsilateral inferior colliculus the MGN in normal adult ferrets receives afferents from other ipsilateral and contralateral brainstem nuclei. Following early extensive removal of its normal afferents, the MGN is reinnervated by novel afferents, including retinal and other non-retinal axons. Removal of normal retinal targets does not increase the extent of retinal projections to the MGN. The diameters of retinal axons innervating the auditory thalamus in lesioned animals suggest that the novel retino-MGN projection might arise from more than one type of retinal ganglion cells.

Factors affecting the establishment and extent of novel retinal projections to the MGN

In the present study, we have shown that availability of terminal space in the MGN is the factor that most influences the formation and quantity of novel retinal projections to this thalamic nucleus. The extent of MGN deafferentation correlated well with the extent of the novel projection, and, as previously demonstrated (Schneider, 1973; Roe et al., 1993), this projection did not form when the MGN was not deafferented, regardless of the extent of removal of normal retinal targets. By contrast, no correlation was observed between the extent of ablation of normal retinal targets (SC, LGN, and PT) and the amount of anomalous retinal connections, even when the MGN was extensively deafferented. Animals that received comparable extents of MGN deafferentation, but different extents of normal retinal target ablation, showed similar amounts of retino-MGN projections. Moreover, our results clearly indicated that ablation of the LGN is not required for retinal axons to sprout into the MGN. Although our findings suggest that the extent of SC removal does not affect the quantity of anomalous retino-MGN projections, it remains unclear whether removal of the SC is necessary for the induction of these projections. As stated earlier, it is technically impossible to perform an extensive deafferentation of the MGN without damaging the overlying SC; thus, this remains a hypothesis at this time. However, innervation of the "deafferented" MGN by novel non-retinal afferents, such as somatosensory and visceral sensory fibers, whose normal targets were not ablated, strongly suggests that abnormal availability of terminal space is by itself sufficient to induce novel projections to an ectopic, denervated nucleus. Consistent with this finding, somatosensory fibers have been redirected to the LGN in rats solely by removing the two eyes, i.e., by exclusively deafferenting the LGN (Asanuma and Stanfield, 1990). Furthermore, it has been reported recently that early bilateral cochlear ablation in ferrets induces some retinal axons to invade the MGN (Pallas and Moore, 1997).

A previous study reported that both factors, removal of normal retinal targets and MGN deafferentation, affect the extent of the novel retino-MGN projection in ferrets (Roe et al., 1993). The discrepancy between the present results and the previous study may be attributed to differences in evaluating the extent of MGN deafferentation. In previous studies, partial removal of normal MGN afferents was achieved by ablating the BIC and/or the iIC (Schneider, 1973; Frost, 1982; Sur et al., 1988; Roe et al., 1993) and was estimated solely by direct examination of the BIC and/or IC lesion. In the present study, we have shown that, similar to the cat MGN (reviewed in Winer, 1992), the normal ferret MGN receives inputs from several brainstem auditory and non-auditory nuclei, including brachial inputs mainly arising from the iIC as well as non-brachial inputs. Intrathalamic injections of retrograde tracers revealed that many inputs still innervated the MGN after unilateral ablation of BIC and IC. Although some of these remaining inputs consisted of fibers spared by the BIC lesion, many were fibers that, in response to the neonatal injury, reached the MGN by means of newly created pathways. One possible explanation for this find-

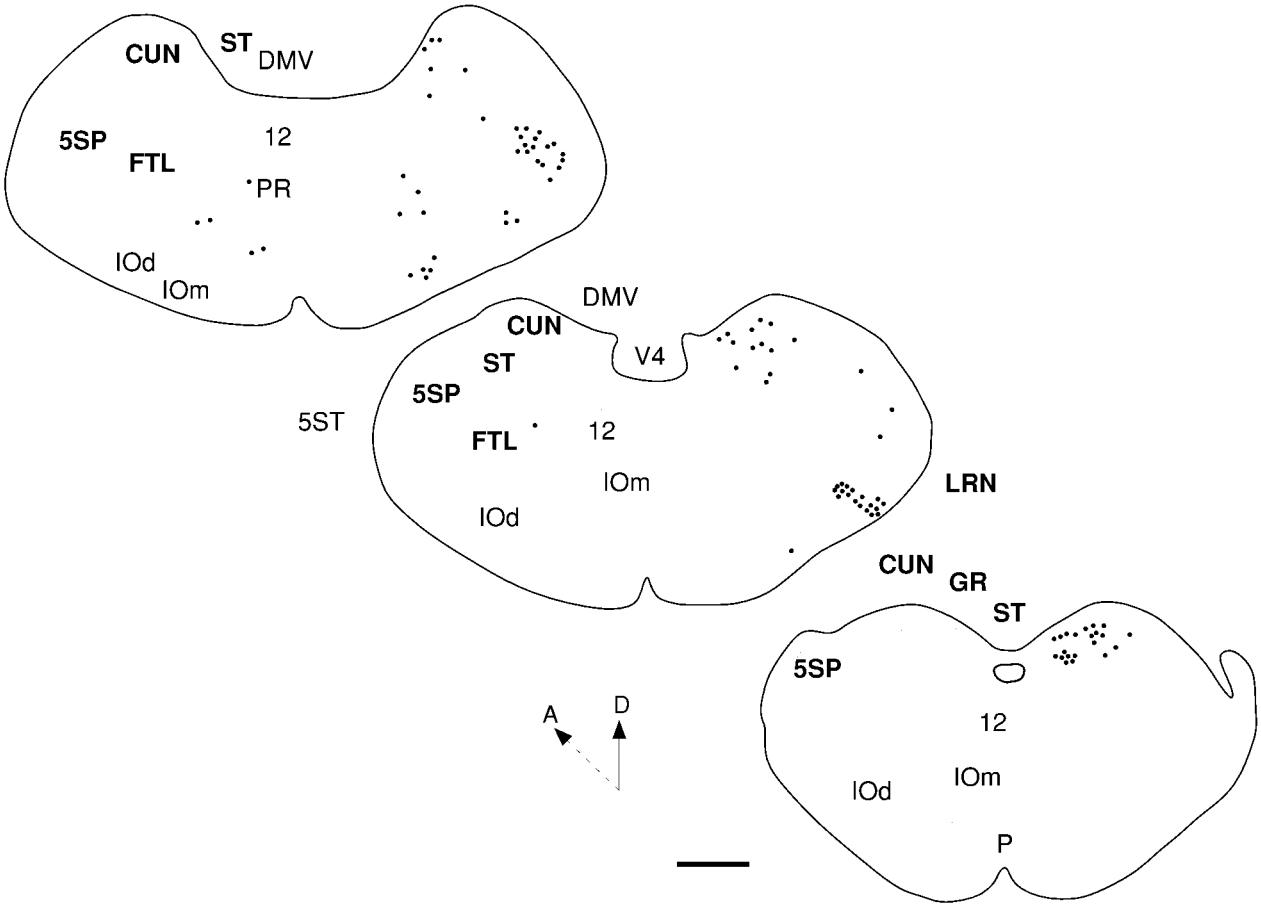

Fig. 13. Novel non-retinal inputs to the medial geniculate nucleus (MGN) after extensive removal of normal auditory MGN afferents. Camera lucida drawings of coronal sections of the medulla in case F96–8 (see Figs. 5, 6), showing cells (dots) retrogradely labeled after an injection of wheat germ agglutinin conjugated to horseradish peroxidase/free horseradish peroxidase in the left MGN (the injection site of this case is shown in Fig. 6). For abbreviations, see list. Scale bar = 1 mm.

TABLE 2. Novel Non-retinal Inputs to the MGN in Lesioned Ferrets: Number of Cells Labeled From an MGN Injection[1]

	GR		CUN		ST		5SP		VN	
Animal	Ipsi	Contra	Ipsi	Contra	Ipsi	Contra	Ipsi	Contra	Ipsi	Contra
Normal	0	0	0	0	0	0	0	0	0	8
F95-23	0	76	4	24	0	156	0	56	0	0
F96-8	16	1224	32	584	4	156	28	164	524	512

[1]CUN, cuneate nucleus; GR, gracile nucleus; MGN, medial geniculare nucleus; ST, nuclei of the solitary tract; VN, vestibular nuclei; 5SP, spinal nucleus of the trigeminal nerve; Contra, contralateral; Ipsi, ipsilateral.

ing is that injured axons were able to regenerate and grow around the injury site by following the course of axons spared by the damage. Consistent with this hypothesis, regeneration of optic, olfactory and pyramidal tract axons after early injury, has been shown to occur in the hamster and rat (Devor, 1975, 1976; Kalil and Reh, 1979; Bernstein and Stelzner, 1981; So et al., 1981; Grafe, 1983). An alternative explanation is that new routes to the MGN were established by ingrowing axons that had not yet reached the MGN at the time of lesion. Thus, our findings clearly show that unilateral removal of BIC and IC is not sufficient to extensively deafferent the auditory thalamus. In contrast, more severe early damage to the ascending auditory pathway, obtained by performing a large transection of the lateral mesencephalon along with ablation of the commissure of the SC and both inferior colliculi, resulted in a marked reduction of auditory brainstem inputs to the MGN, and more extensive novel retinal projections to the auditory thalamus (Fig. 14).

Influence of normal retinal targets on the establishment of anomalous retinal projections to the MGN

Deafferentation of the MGN affected both the induction and amount of novel retino-MGN projections, whereas removal of normal retinal targets did not affect the quantity of the anomalous projection. Paradoxically, our findings seem to suggest that the presence of normal retinal targets is actually necessary for optic tract axons to sprout

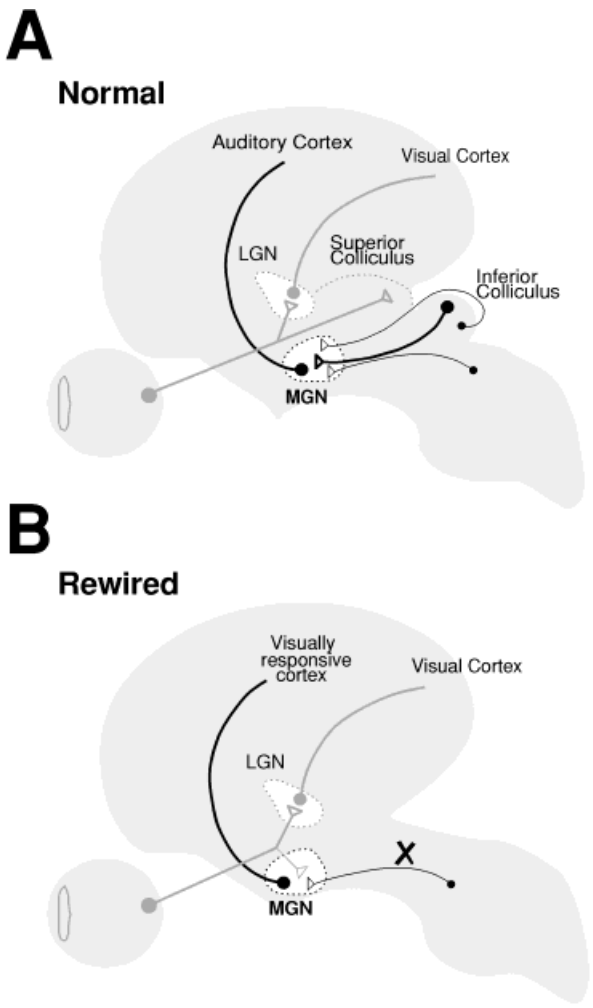

Fig. 14. Summary of the most effective combination of neonatal lesions to induce extensive retinal innervation of the medial geniculate nucleus (MGN). **A:** Visual and auditory pathways in normal ferrets. The visual pathways are shown in gray. The retina projects mainly to the superior colliculus and the lateral geniculate nucleus (LGN). The LGN, in turn, projects to the visual cortex. The auditory pathways are shown in black. Input density is indicated by line thickness. The major source of subcortical inputs to the MGN is the ipsilateral inferior colliculus (thick black line); other inputs arise from the contralateral inferior colliculus (upper thin black line) and from other brainstem nuclei (lower thin black line). The MGN, in turn, projects to the auditory cortex. **B:** Visual and "rewired" pathways in ferrets operated at birth following a new lesion paradigm. Extensive neonatal deafferentation of the MGN, obtained by performing a large transection of the mesencephalon and by lesioning both inferior colliculi as well as the commissure of the superior colliculi, induces retinal fibers to innervate the MGN. A small subset of extrabrachial afferents, arising from several brainstem nuclei, are usually spared by the neonatal lesions and still project to MGN (thin black line). Because the projection from the MGN to the auditory cortex is preserved in lesioned animals, auditory cortex becomes visually responsive. The retino-LGN-visual cortex pathway is preserved in lesioned animals.

into the auditory thalamus. In one case in which complete ablation of LGN and SC, along with extensive removal of PT, was successfully achieved, we observed a marked retrograde degeneration of optic tract fibers and no retinal projections to the MGN. A possible interpretation of this result is that retinal fibers innervating the MGN arise as collaterals of axons directed to normal targets (see Pallas et al., 1994) and that removal of the primary axon prevents the formation of collateral branches into the auditory thalamus. It has been demonstrated that axonal development occurs in two distinct stages (Schneider et al., 1987; Terashima and O'Leary, 1989; Bhide and Frost, 1991; for a review see Jhaveri et al., 1990): axon elongation, during which axons approach their targets, and branch/arbor formation, during which axons invade targets and form terminal arbors. Recent evidence on the targeting behavior of axons has revealed that the permanent projections of neurons are often formed by collateral branches of an initially elongated primary axon, whose distal segment may eventually be eliminated (Stanfield and O'Leary, 1985; Ramoa et al., 1989; for reviews see O'Leary et al., 1990; O'Leary, 1992). Collateralization begins only after, and may be dependent upon, completion of the first stage, i.e., only after axons have reached their most distal target, having already grown past several of the targets to which they will eventually send collateral branches (Schreyer and Jones, 1982; Jhaveri et al., 1983; Schneider et al., 1985; O'Leary and Terashima, 1988; Bhide and Frost, 1991). Current evidence suggests that for some axonal systems, such as the corticopontine (Heffner et al., 1990) and trigeminal (Erzurumlu et al., 1993) axons, the two stages of axonal growth are influenced by different target-derived cues. At the time we perform the surgical manipulations, retinal axons have already invaded their normal targets (Johnson and Casagrande, 1993), have already passed the elongation phase, and have just entered the collateralization/arborization phase, but have terminal arbors that are still very immature and susceptible to extrinsic influences (Hahm et al., 1991). Deafferentation of the MGN might, in a manner similar to that described for other axonal systems (O'Leary et al., 1991; Sato et al., 1994), trigger the release of an as yet unidentified molecule or factor that stimulates axonal collateralization from the primary axon. If the two stages of axon development are susceptible to different extrinsic influences, then elimination of the main axon trunk might prevent collateralization and thus the formation of anomalous connections.

Factors limiting the extent of novel retinal projections to the MGN

Although extensive deafferentation of the MGN consistently induced more extensive retino-MGN projections, retinal fibers could only be induced to innervate approximately 6% of the total MGN volume, or 10% of the rostral half of MGN (including its various subdivisions). Although this information by itself does not suggest that the anomalous retinal axons make functional connections within the novel target, previous studies, in which retinal projections were induced to the MGN by using a slightly different lesion paradigm from that used in this study, indicated that retinal axons establish synaptic contacts within the MGN (Campbell and Frost, 1988) and that cells in the MGN are visually responsive (Roe et al., 1993). One possible factor limiting the extent of retinal innervation of the auditory thalamus may be competition between retinal and other afferent systems for vacated terminal space in the MGN. Consistent with this hypothesis, the "deafferented" MGN was found to receive some normal inputs from auditory and non-auditory brainstem nuclei spared by the neonatal lesions, as well as novel inputs from the retina

and from other sensory nuclei, including somatosensory and visceral nuclei. Support for the hypothesis of competition between afferent axons in the MGN was previously demonstrated by Angelucci et al. (1997) who reported that axons from the two eyes segregate into eye-specific clusters in the MGN of experimentally manipulated ferrets. It is conceivable that the undamaged axons innervating the MGN at the time of lesion have a competitive advantage over retinal and other more distantly located axons. Thus, remnants of normal inputs spared by the lesion might sprout, retain exuberant projections, or fail to retract misplaced collaterals within the MGN in response to partial denervation. Reactive sprouting of normal undamaged afferents, as well as retention of exuberant or misplaced collaterals into a partially denervated target, has been shown previously to occur in several brain regions (Kalil, 1972; Lund, 1972; Lund et al., 1973; Schneider, 1973; Land and Lund, 1979). Moreover, after early coagulation of vibrissa follicles in mice, an increased number of GABA-positive axon terminals (likely arising from the reticular thalamic nucleus) was observed in the ventrobasal thalamic complex (Hámori et al., 1990). Surprisingly, many of these GABA-positive terminals replaced the ablated specific vibrissa afferents, indicating that even axons of different types, that normally occupy different parts of the dendritic tree, can compete for common terminal space. However, our results suggest that innervation of a deafferented target by novel afferents is not a completely non-specific process. The inputs that innervated the MGN after extensive removal of its afferents were either novel lemniscal afferents of a different sensory modality, which normally course in the vicinity of the MGN, or lemniscal and non-lemniscal afferents that normally innervate this nucleus. By contrast, non-lemniscal axons from nuclei that normally do not project to the MGN but are located in its vicinity, such as the substantia nigra, the red nucleus, or other thalamic nuclei such as the ventrobasal complex or the lateral posterior nucleus, did not invade the deafferented MGN.

Recent anatomical data on specific patterns of connections between the cortex and thalamus suggest that another group of axons that might compete with retinal and other lemniscal afferents in the MGN are auditory corticothalamic axons from layer 5. In various thalamic nuclei in normal animals, including the auditory thalamus, cortical layer 5 cells make synaptic contacts onto the proximal dendrites of relay neurons (Ojima, 1994; Guillery, 1995), where subcortical lemniscal afferents also terminate (Majorossy and Réthelyi, 1968; Jones and Powell, 1969; Jones, 1985). In addition, layer 5 auditory corticothalamic axons are about to enter the MGN at the time we perform the surgical manipulation (Clascá et al., 1995). Thus, layer 5 axons could compete for terminal space in the MGN with retinal and other lemniscal afferents, for example by sprouting within the MGN in response to denervation. Anatomical tracing studies would be required to test this hypothesis. An interesting observation of the present study, as well as of a previous study (Angelucci et al., 1997), is that the MGN appeared normal in size after extensive neonatal ablation of its inputs. In the present study, the extent of MGN deafferentation did not correlate with MGN volume, in that cases with more extensive MGN deafferentation did not show greater reduction in MGN volume than cases with less extensive denervation of MGN. This finding is in marked contrast with the severe atrophy of the LGN observed after early binocular enucleation (Guillery et al., 1985a,b; Rakic, 1988; Asanuma and Stanfield, 1990; Brunso-Bechtold and Vinsant, 1990; Dehay et al., 1996). An intriguing hypothesis is that sprouting of the early developing feedback axons from cortical layer 5 might rescue the MGN, deprived of its subcortical inputs, from atrophy. In contrast, neonatal binocular enucleation might result in atrophy of the LGN because this nucleus lacks a projection from cortical layer 5 (Lund et al., 1975; Gilbert and Kelly, 1975; Clascá et al., 1995) and corticogeniculate axons from layer 6 do not invade it until about a week postnatally (McConnell et al., 1994; Clascá et al., 1995).

Besides competition among several afferent systems within the MGN, another possible factor that might limit the extent of retino-MGN projections is the developmental age at which the experimental manipulations are performed (Roe et al., 1993). The first retinogeniculate axons reach their target very early in development, at embryonic day 27 in the ferret, i.e., approximately 14 days before birth (Johnson and Casagrande, 1993). Although data on the time of arrival of afferent axons to the auditory thalamus in the ferret are lacking, studies in other species indicate that most thalamic nuclei are innervated by afferent axons at very early stages of development (Wye-Dvorak, 1984; Martin et al., 1987; Leamey et al., 1996 a,b), and that functional connections are established soon after arrival of the first axons (Leamey et al., 1996a). It is, therefore, possible that at birth, in the ferret, the susceptibility of retinal axons to environmental changes is greatly reduced and that only the latest generated axons can still undergo plastic changes in response to environmental modifications.

Classes of retinal ganglion cells projecting to the MGN

Previous physiological and anatomical results have suggested that under a paradigm that includes lesions of the visual cortex, retino-MGN projections arise from the W-class of retinal ganglion cells (RGCs; Roe et al., 1993; Pallas et al., 1994; Pallas and Sur, 1994). The range of retino-MGN axon diameters found in the present study, which used a lesion paradigm that spared the visual cortex and the LGN, overlaps extensively with the ranges of diameters of X, Y, and W axons in the normal LGN (Roe et al., 1989). However, because measurements of axon caliber in the present study were not made proximally in the optic tract, we cannot exclude the possibility that our axonal population included collateral branches of main axons. Thus, for example, some of the thinner axons in our population, whose caliber appeared to fall within the range of W or X LGN axons, might instead be collaterals of thicker X or Y axons. Although we cannot make conclusive inferences about types and distributions of the retinal ganglion cells that project to MGN, there is little doubt that at least the thickest retino-MGN axons (diameter, 3.6 μm) found in the present study have axon calibers similar to those reported for the thickest retino-LGN Y axons (diameter, 3.7 μm; Roe et al., 1989). Because it is difficult to envisage how modified W or X cells would acquire thicker axon diameters, it is likely that at least some of the retino-MGN axons we have found arise from the Y class of retinal ganglion cells. The discrepancy between our study and the study by Pallas et al. (1994) might be attributed to the different lesion paradigms used in the two studies. It is

well established that in normal cats and experimentally manipulated ferrets, neonatal visual cortical lesions result in marked retrograde degeneration of X-RGCs (Tong et al., 1982; Callahan et al., 1984; Payne et al., 1984; Roe et al., 1993) and medium-sized W-RGCs (Rowe, 1990a; Roe et al., 1993). Moreover, after neonatal visual cortical lesions, Y-RGCs show reduced soma size (Rowe, 1990a) and conduction velocity (Rowe, 1990b) as well as altered axon arbor morphology in the LGN (Weber et al., 1986). Thus, it is possible that only small W-cells and modified Y-cells survived in the retinae of ferrets that received neonatal ablation of the visual cortex (Roe et al., 1993; Pallas et al., 1994). Physiological and further anatomical studies would be required to characterize in detail which RGC types innervate the MGN under our new lesion paradigm.

CONCLUSIONS

We have shown that the abnormal availability of terminal space in the MGN is the main factor affecting the formation and quantity of anomalous retino-MGN projections. However, we have also shown that the retina cannot entirely take over this novel target. Our findings suggest that the factor that appears necessary for the induction of anomalous retinal projections might paradoxically be the same factor that limits the quantity of these projections, namely competition among different sets of afferent systems for terminal synaptic space.

ACKNOWLEDGMENTS

We thank S. Kuffler for technical assistance, Dr. R.P. Marini for assistance with surgical procedures, Drs. P. Kind and J. B. Levitt for helpful comments on the manuscript, and Dr. E. Bricolo for writing computer software for data analysis. We are also grateful to Dr. A.W. Roe for an injection case. M.S. received grant support from the National Institutes of Health and the March of Dimes, and F.C. received grant support from Fogarty International Fellowship.

LITERATURE CITED

Angelucci, A., F. Clascá, and M. Sur (1996) Anterograde axonal tracing with the subunit B of cholera toxin: A highly sensitive immunohistochemical protocol for revealing fine axonal morphology in adult and neonatal brains. J. Neurosci. Methods *65:*101–112.

Angelucci, A., F. Clascá, E. Bricolo, K.S. Cramer, and M. Sur (1997) Experimentally induced retinal projections to the ferret auditory thalamus: Development of clustered eye-specific patterns in a novel target. J. Neurosci. *17:*2040–2055.

Asanuma, C. and B.B. Stanfield (1990) Induction of somatosensory inputs to the lateral geniculate nucleus in congenitally blind mice and in phenotypically normal mice. Neuroscience *39:*533–545.

Berman, A.L. (1968) The Brainstem of the Cat. A Cytoarchitectonic Atlas With Stereotaxic Coordinates. Wisconsin: University of Wisconsin Press.

Berman, A.L. and E.G. Jones (1982) The Thalamus and Basal Telencephalon of the Cat. A Cytoarchitectonic Atlas With Stereotaxic Coordinates. Wisconsin: University of Wisconsin Press.

Bernstein, D. and D. Stelzner (1981) Corticospinal tract (CST) plasticity in the early postnatal rat. Soc. Neurosci. Abstr. *7:*678.

Bhide, P.G. and D.O. Frost (1991) Stages of growth of hamster retinofugal axons: Implications for developing axonal pathways with multiple targets. J. Neurosci. *11:*485–504.

Brunso-Bechtold, J.K. and S.L. Vinsant (1990) An ultrastructural and morphometric study of the effect of removal of retinal input on the development of the dorsal lateral geniculate nucleus. J. Comp. Neurol. *301:*585–603.

Callahan, E.C., L. Tong, and P.D. Spear (1984) Critical period for the marked loss of retinal X-cells following visual cortex damage in cats. Brain Res. *323:*302–306.

Campbell, G. and D.O. Frost (1988) Synaptic organization of anomalous retinal projections to the somatosensory and auditory thalamus: Target-controlled morphogenesis of axon terminals and synaptic glomeruli. J. Comp. Neurol. *272:*383–408.

Clascá, F., A. Angelucci, and M. Sur (1995) Layer-specific programs of development in neocortical projection neurons. Proc. Natl. Acad. Sci. USA *92:*11145–11149.

Dehay, C., P. Giroud, M. Berland, H. Killackey, and H. Kennedy (1996) Contribution of thalamic input to the specification of cytoarchitectonic cortical fields in the primate: Effects of bilateral enucleation in the fetal monkey on the boundaries, dimensions, and gyrification of striate and extrastriate cortex. J. Comp. Neurol. *367:*70–89.

Devor, M. (1975) Neuroplasticity in the sparing or deterioration of function after early olfactory tract lesions. Science *190:*998–1000.

Devor, M. (1976) Neuroplasticity in the rearrangement of olfactory tract fibers after neonatal transection in hamsters. J. Comp. Neurol. *166:* 31–48.

Erzurumlu, R.S., S. Jhaveri, H. Takahashi, and R.D.G. McKay (1993) Target-derived influences on axon growth modes in cultures of trigeminal neurons. Proc. Natl. Acad. Sci. USA *90:*7235–7239.

Frost, D.O. (1981) Orderly anomalous retinal projections to the medial geniculate, ventrobasal, and lateral posterior nuclei of the hamster. J. Comp. Neurol. *203:*227–256.

Frost, D.O. (1982) Anomalous visual connections to somatosensory and auditory systems following brain lesions in early life. Dev. Brain Res. *3:*627–635.

Frost, D.O. (1986) Development of anomalous retinal projections to non-visual thalamic nuclei in Syrian hamsters: A quantitative study. J. Comp. Neurol. *252:*95–105.

Gilbert, C.D. and J.P. Kelly (1975) The projections of cells in different layers of the cat's visual cortex. J. Comp. Neurol. *163:*81–105.

Grafe, M. (1983) Developmental factors affecting regeneration in the central nervous system: Early but not late formed mitral cells reinnervate olfactory cortex after neonatal tract section. J. Neurosci. *3:*617–630.

Graziadei, P.P.C., R.R. Levine, and G.A. Monti-Graziadei (1979) Plasticity of connections of the olfactory sensory neuron: Regeneration into the forebrain following bulbectomy in the neonatal mouse. Neuroscience *4:*713–727.

Guillery, R.W. (1995) Anatomical evidence concerning the role of the thalamus in cortico-cortical communication: A brief review. J. Anat. *187:*583–592.

Guillery, R.W., A.L. LaMantia, J.A. Robson, and K. Huang (1985a) The influence of retinal afferents upon the development of layers in the dorsal lateral geniculate nucleus of mustelids. J. Neurosci. *5:*1370–1379.

Guillery, R.W., M. Ombrellaro, and A.L. LaMantia (1985b) The organization of the lateral geniculate nucleus and of the geniculocortical pathway that develops without retinal afferents. Brain Res. *352:*221–233.

Hahm, J.-O., R.B. Langdon, and M. Sur (1991) Disruption of retinogeniculate afferent segregation by antagonists to NMDA receptors. Nature *351:*568–570.

Hámori, J., J. Takács, R. Verley, P. Petrusz, and E. Farkas-Bargeton (1990) Plasticity of GABA- and glutamate-containing terminals in the mouse thalamic ventrobasal complex deprived of vibrissal afferents: An immunogold-electron microscopic study. J. Comp. Neurol. *302:*739–748.

Heffner, C.D., A.G.S. Lumsden, and D.D.M. O'Leary (1990) Target control of collateral extension and directional axon growth in the mammal brain. Science *247:*217–220.

Jhaveri, S., M.A. Edwards, and G.E. Schneider (1983) Two stages of growth during development of the hamster's optic tract. Anat. Rec. *205:*225.

Jhaveri, S., M.A. Edwards, R.S. Erzurumlu, and G.E. Schneider (1990) Elongation and arborization of CNS axons. In N.M. Van Gelder, R.F. Butterworth, and B.D. Drujan (eds): (Mal)Nutrition and the Infant Brain. New York: Wiley-Liss, pp. 111–125.

Johnson, J.K. and V.A. Casagrande (1993) Prenatal development of axon outgrowth and connectivity in the ferret visual system. Vis. Neurosci. *10:*117–130.

Jones, E.G. (1985) The Thalamus. New York: Plenum Press.

Jones, E.G. and T.P.S. Powell (1969) Electron microscopy of synaptic glomeruli in the thalamic relay nuclei of the cat. Proc. R. Soc. Lond. B *172:*153–171.

Kalil, R.E. (1972) Formation of new retinogeniculate connections in kittens after removal of one eye. Anat. Rec. *172:*339–340.

Kalil, R.E. and T. Reh (1979) Regrowth of severed axons in the neonatal central nervous system: Establishment of normal connections. Science *205:*1158–1161.

Land, P.W. and R.D. Lund (1979) Development of the rat's uncrossed retinotectal pathway and its relation to plasticity studies. Science *205:*698–700.

Leamey, C.A., S.M. Ho, and R.F. Mark (1996a) Afferent arrival and onset of functional activity in the trigeminothalamic pathway of the rat. Soc. Neurosci. Abstr. *22:*758.

Leamey, C.A., L.R. Marotte, and P.M.E. Waite (1996b) Timecourse of development of the wallaby trigeminal pathway: II. Brainstem to thalamus and the emergence of cellular aggregations. J. Comp. Neurol. *364:*494–514.

Lund, R.D. (1972) Anatomic studies on the superior colliculus. Invest. Ophthalmol. *11:*434–441.

Lund, R.D., T.S. Cunningham, and J.S. Lund (1973) Modified optic pathways after unilateral eye removal in young rats. Brain Behav. Evol. *8:*51–72.

Lund, J.S., R.D. Lund, A.E. Hendrickson, A.H. Bunt, and F. Fuchs (1975) The origin of efferent pathways from the primary visual cortex, area 17, of the macaque monkey as shown by retrograde transport of horseradish peroxidase. J. Comp. Neurol. *164:*287–304.

Majorossy, K. and M. Réthelyi (1968) Synaptic architecture in the medial geniculate body (ventral division). Exp. Brain Res. *6:*306–323.

Martin, G.F., T. Cabana, J.C. Hazlett, R. Ho, and R. Waltzer (1987) Development of brainstem and cerebellar projections to the diencephalon with notes on thalamocortical projections: Studies in the North American opossum. J. Comp. Neurol. *260:*186–200.

McConnell, S.K., A. Ghosh, and C.J. Shatz (1994) Subplate pioneers and the formation of descending connections from cerebral cortex. J. Neurosci. *14:*1892–1907.

Mesulam, M.M. (1978) Tetramethyl benzidine for horseradish peroxidase neurohistochemistry: A non-carcinogenic blue reaction product with superior sensitivity for visualizing neural afferents and efferents. J. Histochem. Cytochem. *26:*106–117.

Ojima, H. (1994) Terminal morphology and distribution of corticothalamic fibers originating from layers 5 and 6 of cat primary auditory cortex. Cereb. Cortex *6:*646–663.

O'Leary, D.D.M. (1992) Development of connectional diversity and specificity in the mammalian brain by the pruning of collateral projections. Curr. Opin. Neurobiol. *2:*70–77.

O'Leary, D.D.M. and T. Terashima (1988) Cortical axons branch to multiple subcortical targets by interstitial axon budding: Implications for target recognition and "waiting periods." Neuron *1:*901–910.

O'Leary, D.D.M., A.R. Bicknese, J.A. De Carlos, C.D. Heffner, S.E. Koester, L.J. Kutka, and T. Terashima (1990) Target selection by cortical axons: Alternative mechanisms to establish axonal connections in the developing brain. Cold Spring Harb. Symp. Quant. Biol. *55:*153–468.

O'Leary, D.D.M., C.D. Heffner, L. Kutka, L. Lopez-Mascaraque, A. Missias, and B.S. Reinoso (1991) A target derived chemoattractant controls the development of the corticopontine projection by a novel mechanism of axon targeting. Development Suppl. *2:*123–130.

Pallas, S.L. and D.R. Moore (1997) Retinal axons arborize in the medial geniculate nucleus of neonatally-deafened ferrets. Soc. Neurosci. Abstr. *23:*1994.

Pallas, S.L. and M. Sur (1994) Morphology of retinal axons induced to arborize in a novel target, the medial geniculate nucleus: II. Comparison with arbors from the inferior colliculus. J. Comp. Neurol. *349:*363–376.

Pallas, S.L., J.-H. Hahm, and M. Sur (1994) Morphology of retinal axons induced to arborize in a novel target, the medial geniculate nucleus: I. Comparison with arbors in normal targets. J. Comp. Neurol. *349:*343–362.

Payne, B.R., H.E. Pearson, and P. Cornwell (1984) Transneuronal degeneration of beta retinal ganglion cells in the cat. Proc. R. Soc. Lond. B *222:*15–32.

Rakic, P. (1988) Specification of cerebral cortical areas. Science *241:*170–176.

Ramoa, A.S., G. Campbell, and C.J. Shatz (1989) Retinal ganglion § cells project transiently to the superior colliculus during development. Proc. Natl. Acad. Sci. USA *86:*2061–2065.

Roe, A.W., P.E. Garraghty, and M. Sur (1989) Terminal arbors of single ON-center and OFF-center retinal ganglion cell axons within the ferret's lateral geniculate nucleus. J. Comp. Neurol. *228:*208–242.

Roe, A.W., P.E. Garraghty, M. Esguerra, and M. Sur (1993) Experimentally induced visual projections to the auditory thalamus: Evidence for a W cell pathway. J. Comp. Neurol. *334:*263–280.

Rowe, M.H. (1990a) Evidence for degeneration of retinal W cells following early visual cortical removal in cats. Brain Behav. Evol. *35:*253–267.

Rowe, M.H. (1990b) Reduced conduction velocity of retinal Y-cell axons following early partial removal of their synaptic targets. Brain Res. *514:*119–127.

Sato, M., L. Lopez-Mascaraque, C.D. Heffner, and D.D.M. O'Leary (1994) Action of a diffusible target-derived chemoattractant on cortical axon branch induction and directed growth. Neuron *13:*791–803.

Schneider, G.E. (1973) Early lesions of superior colliculus: Factors affecting the formation of abnormal retinal projections. Brain Behav. Evol. *8:*73–109.

Schneider, G.E., S. Jhaveri, M.A. Edwards, and K.-F. So (1985) Regeneration, re-routing, and redistribution of axons after early lesions: Changes with age, and functional impact. In J.C. Eccles and M. Dimitrijevic (eds): Recent Achievements In Restorative Neurology 1: Upper Motor Neuron Functions and Dysfunctions. New York: Karger, pp. 291–310.

Schneider, G.E., S. Jhaveri, and W. Davis (1987) On the development of neuronal arbors. In C. Chagas and R. Linden (eds): Developmental Neurobiology of Mammals. Vatican City: Pontifical Academy of Sciences, pp. 31–64.

Schreyer, D.J. and E.G. Jones (1982) Growth and target finding by axons of the corticospinal tract in prenatal and postnatal rats. Neuroscience *8:*1837–1853.

So, K.-F., G.E. Schneider, and S. Ayres (1981) Lesions of the brachium of the superior colliculus in neonate hamsters: Correlation of anatomy with behavior. Exp. Neurol. *72:*379–400.

Stanfield, B.B. and D.D.M. O'Leary (1985) The transient corticospinal projection from the occipital cortex during postnatal development in the rat. J. Comp. Neurol. *238:*236–248.

Sur, M., P.E. Garraghty, and A.W. Roe (1988) Experimentally induced visual projections into auditory thalamus and cortex. Science *242:*1437–1441.

Terashima, T. and D.D.M. O'Leary (1989) Growth and branching of cortical axons: Implications for target selection by developing axons. Soc. Neurosci. Abstr. *15:*875.

Tong, L., P.D. Spear, R.E. Kalil, and E.C. Callahan (1982) Loss of retinal X-cells in cats with neonatal or adult visual cortex damage. Science *217:*72–75.

Weber, A.J., R.E. Kalil, and L.R. Stanford (1986) Morphology of single, physiologically identified retinogeniculate Y-cell axons in the cat following damage to visual cortex at birth. J. Comp. Neurol. *282:*446–455.

Winer, J.A. (1992) The functional architecture of the medial geniculate body and the primary auditory cortex. In D.D. Webster, A.N. Popper, and R.R. Fay (eds): The Mammalian Auditory Pathway: Neuroanatomy. New York: Springer-Verlag, pp. 222–409.

Wong-Riley, M.T.T. (1979) Changes in the visual system of monocularly sutured or enucleated cats demonstrated with cytochrome oxidase histochemistry. Brain Res. *17:*11–28.

Wye-Dvorak, J. (1984) Postnatal development of primary visual projections in the tammar wallaby (*Macropus eugenii*). J. Comp. Neurol. *228:*491–508.